Studies on Therapeutic Targets for Type 2 Diabetes Using Small-molecule Ligands

A Dissertation Submitted to
the Graduate School of Life and Environmental Science,
the University of Tsukuba
in Partial Fulfillment of the Requirements
for the Degree of Doctor of Philosophy in Biological Science
(Doctoral Program in Biological Science)

Takehiro TAKAHASHI

Abbreviations

AUC: areas under the curve

BVT116429: (S)-2-((S)-1-(2-fluorophenyl)ethylamino)-5-methyl-5-(trifluoromethyl) thiazol-4(5H)-one

BVT2733: 3-chloro-2-methyl-N-[4-[2-(4-methylpiperazin-1-yl)-2-oxoethyl]-1,3-thiazol-2-yl] benzenesulfonamide

CBX: carbenoxolone, (3β)-3-[(3-carboxypropanoyl)oxy]-11-oxoolean-12-en-30-oic acid

Cpd544: compound 544, 3-[(1s,3s)-adamantan-1-yl]-6,7,8,9-tetrahydro-5H-[1,2,4]triazolo[4,3-a]azepine

DIO: diet induced obesity

DMSO: dimethyl sulfoxide

HFD: high fat diet

HIS-388: N-[(1R,2s,3S,5s,7s)-5-hydroxyadamantan-2-yl]-3-(pyridin-2-yl) isoxazole-4-carboxamide

HOMA-IR: homeostasis model assessment-insulin resistance

HTRF: homogenous time resolved fluorescence

IC_{50}: half maximal (50%) inhibitory concentration

IL-6: interleukin-6

ITT: insulin tolerance test

KR-66344: 2-(3-benzoyl)-4-hydroxy-1,1-dioxo-2H-1,2-benzothiazine-2-yl-1-phenylethanone

MS: microsomes

mtDNA: mitochondrial DNA

OGTT: oral glucose tolerance test

PCR: polymerase chain reaction

PGC-1α: peroxisome proliferator activated receptor-γ coactivator-1α

Pioglitazone: 5-[[4-[2-(5-ethylpyridin-2-yl)ethoxy]phenyl]methyl]-1,3-thiazolidine-2,4-dione

PPARγ: peroxisome proliferator-activated receptor-γ

PTT: pyruvate tolerance test

RU: resonance unit

S.E.M.: standard error of mean

SPR: surface plasmon resonance

STZ: streptozotocin

TNF-α: tumor necrosis factor-α

TR-FRET: time-resolved fluorescence resonance energy transfer

TT01001: ethyl-4-(3-(3,5-dichlorophenyl)thioureido)piperidine-1-carboxylate

11β-HSD1: 11β-Hydroxysteroid dehydrogenase type 1

Contents

Abstract

The prevalence of type 2 diabetes has dramatically increased in recent years, causing a global burden. Type 2 diabetes is characterized by impaired insulin secretion from pancreatic β cells and insulin resistance in the liver, muscle, and adipose tissue. Notably, insulin resistance is one of the important causes and a key feature of type 2 diabetes. Thus, improvement of insulin resistance is effective for the treatment of type 2 diabetes. Pioglitazone, peroxisome proliferator-activated receptor-γ (PPARγ) agonist has been known as potent insulin sensitizer and widely used for the treatment of type 2 diabetes in the world. However, pioglitazone exhibits considerable side effects, weight gain or edema, thus clinical use of it in patients with heart failure, a past history of heart failure, or renal dysfunction has been limited. So, it is important to explore novel compounds which show potent antidiabetic effects without considerable side effects is useful for the future treatment of type 2 diabetes.

A mitochondrial outer membrane protein mitoNEET is a binding protein of pioglitazone and is considered a novel target for the treatment of type 2 diabetes. Several small-molecule compounds have been identified as mitoNEET ligands using structure-based design or virtual docking studies. However, there are no reports about their therapeutic potential in animal models. Recently, TT01001 was synthesized as a novel small molecule, designed on the basis of pioglitazone structure. In chapter 1, I assessed the pharmacological properties of TT01001 in both *in vitro* and *in vivo* studies. I found that TT01001 bound to mitoNEET without PPARγ activation effect. In type 2 diabetes model db/db mice, TT01001 improved hyperglycemia, hyperlipidemia, and glucose intolerance, and its efficacy was equivalent to that of pioglitazone, without the pioglitazone-associated weight gain. Mitochondrial complexes II+III activity of the skeletal muscle was significantly increased in db/db mice. I also found that TT01001 significantly suppressed the elevated activity of the complexes II+III. These results suggest that TT01001 improved type 2 diabetes without causing weight gain and

ameliorated mitochondrial function of db/db mice. This is the first study that demonstrates the effects of a mitoNEET ligand on glucose metabolism and mitochondrial function in an animal disease model.

11β-Hydroxysteroid dehydrogenase type 1 (11β-HSD1) is considered a potential therapeutic target in the treatment of type 2 diabetes mellitus. In chapter 2, I investigated the pharmacological properties of HIS-388, a newly synthesized 11β-HSD1 inhibitor, using several mouse models. In cortisone pellet-implanted mice in which hypercortisolism and hyperinsulinemia occur, single administration of HIS-388 exhibited potent and prolonged suppression of plasma cortisol and lowered plasma insulin levels. These effects were more potent than those achieved using the same dose of other 11β-HSD1 inhibitors (carbenoxolone and compound 544), indicating that HIS-388 potently and continuously suppresses 11β-HSD1 enzyme activity *in vivo*. In diet-induced obese (DIO) mice, HIS-388 significantly decreased fasting blood glucose, plasma insulin concentration, and homeostasis model assessment-insulin resistance (HOMA-IR) score, and ameliorated insulin sensitivity. In addition, HIS-388 significantly reduced body weight and suppressed the elevation of blood glucose during the pyruvate tolerance test. In non-genetic type 2 diabetic mice with disease induced by a high-fat diet and low-dose streptozotocin, HIS-388 also significantly decreased postprandial blood glucose and plasma insulin levels and improved glucose intolerance. The effects of HIS-388 on glucose metabolism were indistinguishable from those of an insulin sensitizer, pioglitazone. These results suggest that HIS-388 is a potent agent against type 2 diabetes. Moreover, amelioration of diabetic symptoms by HIS-388 was at least in part attributable to an antiobesity effect or improvement of hepatic insulin resistance. Therefore, potent and long-acting inhibition of 11β-HSD1 enzyme activity may be an effective approach for the treatment of type 2 diabetes and obesity associated disease. These studies would support targeting mitoNEET and 11β-HSD1 as a useful therapeutic approach for the future treatment of type 2 diabetes.

General Introduction

Diabetes is one of the most common chronic diseases, and its prevalence has dramatically increased in recent years (Whiting *et al*., 2011). In a general classification, diabetes is divided into two groups, type 1 diabetes and type 2 diabetes. Type 1 diabetes is called insulin dependent diabetes mellitus, and it is an autoimmune disease that leads to destruction of pancreatic β-cell, which results in a complete depletion of insulin production (van Belle *et al*., 2011). Meanwhile, type 2 diabetes is also called non-insulin dependent diabetes mellitus, and accounts for about 90 to 95 percent of all diabetic patients. Type 2 diabetes is characterized by resistance to the action of insulin on peripheral tissue, such as skeletal muscle, liver or adipose tissue (Kahn *et al*., 2006). This phenomenon is known as "insulin resistance". Insulin resistance is a key feature of type 2 diabetes and is defined as a state in which more than normal levels of insulin are required to obtain biologic effects (Ruderman *et al*., 2013). The cause of insulin resistance is not fully understood, while many metabolic dysfunctions may be associated with it. Obesity which is characterized by excess adipose tissue with infiltration of activated macrophages is one of the common contributing factors in the development of insulin resistance. Activated macrophages in adipose tissue secrete inflammatory adipocytokines, such as tumor necrosis factor-α (TNF-α) and interleukin-6 (IL-6), which contribute to insulin resistance (Kadowaki *et al*., 2006). Intracellular lipid accumulation in peripheral tissue, skeletal muscle or liver is also associated with impaired insulin sensitivity *via* alteration of insulin receptor signal (Corcoran *et al*., 2007; Perry *et al*., 2014). Insulin resistance results in compensatory hyperinsulinemia, leading to pancreatic β-cell dysfunction, hyperglycemia and glucose intolerance (Abdul-Ghani *et al*., 2006). Therefore, improvement of insulin resistance is considered to be effective strategies for the treatment of type 2 diabetes.

Many oral drugs have been used in the treatment of type 2 diabetes, such as sulfonylureas, glinides, α-glucosidase inhibitors, incretins, sodium-glucose cotransporter 2 inhibitors, biguanides and thiazolidinediones (Padwal *et al*., 2005, Brunton, 2015). Notably, thiazolidinediones derivative, pioglitazone has been known as potent insulin sensitizer for the treatment of type 2 diabetes (Ahmadian *et al*., 2013). Pioglitazone decreases serum triglycerides, free fatty acids, and inflammatory adipocytokines, TNF-α and IL-6, and increases the insulin-sensitizing hormone adiponectin by activating peroxisome proliferator-activated receptor-γ (PPARγ) (Kadowaki *et al*., 2006; Quinn *et al*., 2008). These various effects of pioglitazone *via* the activation of PPARγ lead to the improvement of insulin resistance and glycemic parameters. Meanwhile, clinical side effects, such as weight gain or edema, are frequently observed in patients with type 2 diabetes treated with pioglitazone and are attributed to PPARγ activation (Tang and Maroo, 2007; Borsting *et al*., 2012). So, clinical use of pioglitazone has been limited in patients with heart failure or a past history of heart failure or renal dysfunction (Nissen and Wolski, 2007). Therefore, it has been thought that the exploration of novel compounds which show potent antidiabetic effects without considerable side effects is important for the future treatment of type 2 diabetes.

In this study, I focused on the two candidate targets of type 2 diabetes, mitochondrial outer membrane protein mitoNEET and glucocorticoid activating enzyme 11β-hydroxysteroid dehydrogenase type 1 (11β-HSD1), and investigated their usefulness for the treatment of type 2 diabetes using novel small-molecule ligands, respectively. To reveal the usefulness of these targets, first, I assessed the pharmacological profiles of TT01001, which is a novel ligand designed on the basis of insulin sensitizer pioglitazone structure, in both *in vitro* and disease animal model studies. Second, I investigated the *in vivo* pharmacological properties of HIS-388, which is a novel 11β-HSD1 inhibitor, in several disease animal models.

Chapter 1: Pharmacological Properties of TT01001, a novel mitoNEET ligand

1.1. Introduction

Mitochondria are known as the intracellular powerhouse of cells, and mitochondrial dysfunction is involved in a broad spectrum of diseases, both inherited and acquired (Andreux *et al*., 2013). In type 2 diabetes, many studies have focused on the association between the pathology of diabetes and mitochondrial dysfunction. Lower oxidative phosphorylation capacity was observed in muscle biopsy samples of patients with type 2 diabetes compared with those of healthy individuals (Kelley *et* al., 2002; Phielix *et al*., 2008; Ritov *et al*., 2010). The frequent reduction of mitochondrial contents was also shown in patients with type 2 diabetes (Hwang *et al*., 2010; Chomentowski *et al*., 2011). These reports indicate that mitochondrial function plays a key role in the pathology of type 2 diabetes. Recently, several reports have suggested that the pioglitazone directly influences mitochondrial function. For example, pioglitazone inhibits rat mitochondrial complex I activity in the skeletal muscle and liver tissue, indicating that alterations of cellular energy state by pioglitazone may contribute to the improvement in insulin sensitivity (Brunmair *et al*., 2004). Pioglitazone also increases the levels of the mitochondrial biogenesis regulator protein peroxisome proliferator-activated receptor-γ coactivator-1α (PGC-1α) in the skeletal muscle of db/db mice (Pagel-Langenickel *et al*., 2008). In patients with type 2 diabetes, pioglitazone treatment increases both mitochondrial DNA (mtDNA) copy numbers and the expression of PGC-1α in subcutaneous adipose tissue (Bogacka *et al*., 2005). These effects of pioglitazone are speculated to be independent of PPARγ activation (Feinstein *et al*., 2005). The mitochondrial outer membrane protein mitoNEET was identified as a novel binding protein of pioglitazone and has been considered a new target for type 2 diabetes therapies (Colca *et al*., 2004). Although the physiologic role of mitoNEET remains unclear, it is likely to modulate glucose metabolism or mitochondrial function. The mitochondria

isolated from the heart of mitoNEET-deficient mice showed a decrease in state 3 respirations (Wiley *et al*., 2007). Overexpression of mitoNEET inside the adipose cell in genetic type 2 diabetic model ob/ob mice improved glycemic parameters and altered mitochondrial functions (Kusminski *et al*., 2012). Suppressed expression of mitoNEET *in vitro* decreased mitochondrial abilities (Sohn *et al*., 2013). Interestingly, the ligand for mitoNEET, NL-1, suppresses rotenone-induced toxicity in neuronal cells and mildly uncouples mitochondria (Geldenhuys *et al*., 2010). Other ligands for mitoNEET have also been reported by use of virtual docking studies (Bieganski and Yarmush, 2011). However, the *in vivo* effects of glucose metabolism or mitochondrial function have not been clarified for these mitoNEET ligands. Recently, TT01001 was synthesized as an orally active, small molecule that is designed on the basis of the pioglitazone structure. In chapter 1, I first assessed the *in vitro* pharmacological profiles of TT01001 with PPARγ activity and mitoNEET binding. Next, I examined the *in vivo* effects of TT01001 on diabetes and mitochondrial function using the type 2 diabetes murine model, db/db mice.

1.2. Materials & Methods

1.2.1. Chemicals

The TT01001 (Fig. 1-1) was synthesized by the Pharmaceutical Laboratories, Toray Industries, Inc. (Kanagawa, Japan). Pioglitazone hydrochloride (Fig. 1-1) was purchased from Kemprotec Limited (Middlesbrough, Cambria, UK). All compounds were dissolved in dimethyl sulfoxide (DMSO) (Sigma-Aldrich Japan, Tokyo, Japan) for *in vitro* studies, or suspended in 0.5% (w/v) methylcellulose (Nakarai Tesque, Kyoto, Japan) for *in vivo* studies.

1.2.2. mitoNEET Protein Expression and Purification

The protein expression and purification of the soluble human mitoNEET was performed as described previously with slight modification (Zuris *et al*., 2011). The gene of human mitoNEET (human kidney cDNA; Clontech, MountainView, CA) was amplified by polymerase chain reaction (PCR) and cloned to the pCI-neo vector (Promega, Osaka, Japan). The fragment of mitoNEET encoding residues 33-108 was inserted into the pET-28b (+) vector (Novagen, Madison, WI) *via* the *Nde*I and *Xho*I sites, and the expression vector was introduced into *Escherichia coli* BL21 (DE3) cells. The mitoNEET protein was induced by the histidine-tagged protein by adding isopropyl-1-thio-β-D-galactoside (final concentration, 0.5 mmol/L) and culturing for 4 hours at 37°C. The *E. coli* pellets were collected and lysed by sonication in buffer A [50 mmol/L Tris-hydrochloride (HCl) (pH 8.0), 250 mmol/L NaCl, 5 mmol/L imidazole] with 1 mmol/L phenylmethylsulfonyl fluoride. The clarified supernatant was loaded onto a HisTrap HP (GE Healthcare, Tokyo, Japan) column pre-equilibrated with buffer A. The column was washed with buffer A, containing 100 mmol/L imidazole, and the histidine-tagged mitoNEET protein was eluted with buffer A, containing 500 mmol/L imidazole. To remove the histidine tag, the protein solution was incubated with restriction-grade thrombin (Novagen, Madison, WI) for 6 hours at room

temperature. The solution was loaded onto a HiTrap-Benzamidine tandem column (HisTrap HP and HiTrap Benzamidine FF; GE Healthcare, Tokyo, Japan), and the column was washed with the buffer containing 50 mmol/L Tris-HCl (pH 8.0), 50 mmol/L NaCl, and 100 mmol/L imidazole. The flow-through and washing fractions were collected, and the protein was purified by size exclusion chromatography (HiLoad 16/60 Superdex 200 prep grade; GE Healthcare, Tokyo, Japan) in 50 mmol/L Tris-HCl (pH 8.0), 50 mmol/L NaCl.

1.2.3. Time-Resolved Fluorescence Resonance Energy Transfer Assay

The PPARγ activation effect was assessed by the time-resolved fluorescence resonance energy transfer (TR-FRET) method using the LanthaScreen™ TR-FRET PPARγ coactivator assay kit (Invitrogen, Carlsbad, CA). TT01001 or pioglitazone (test compounds) or solvent vehicle (DMSO) was incubated together with the human PPARγ ligand-binding domain tagged with glutathione S-transferase, terbium-labeled anti-glutathione S-transferase antibody, and fluorescein peptide with assay buffer. When binding of the test compound caused a conformational change in the PPARγ ligand binding domain, excitation of terbium at 340 nm resulted in energy transfer and excitation of the fluorescein peptide, followed by emission at 520 nm. The signal at 520 nm was normalized by the signal obtained at 495 nm. Each assay was performed in quadruplicate and the data were expressed as the mean ratios of 520 and 495 nm. The mean ratios were plotted against the concentration of the test compounds.

1.2.4. Surface Plasmon Resonance Interaction Analysis

The surface plasmon resonance (SPR) measurements were carried out by the Biacore S51 instrument (Biacore AB, Uppsala, Sweden). The mitoNEET protein was immobilized onto the sensor chip (CM-5; GE Healthcare, Tokyo, Japan) using the amine coupling method. Different

concentrations of TT01001 (1, 2, 4, 8, and 20 μmol/L) and pioglitazone (0.3, 0.6, 1.3, 2.5, and 5.0 μmol/L) were injected for 60 seconds at a flow rate of 30 μL/min. The resonance unit (RU) curves were normalized by the reference surface and no response concentration using S51 evaluation software (GE Healthcare, Tokyo, Japan).

1.2.5. Animals and Administration of Compounds

This study was reviewed by the Animal Care and Use Committee, approved by the head of the test facility, and performed in accordance with the Guidelines for Animal Experiments, Research and Development Division, Toray Industries, Inc. Male, 5-week-old mice of C57BL/6J and BKS. Cg-+*Leprdb*/+*Leprdb* (db/db) were obtained from CLEA Japan, Inc. (Tokyo, Japan). All mice were group-housed in cages at 22-24°C with a 12-hour light/dark cycle (lights on at 7:00 AM) for 1 week before the experiments began. Mice were given *ad libitum* access to food and water. In db/db mice, the vehicle (0.5% methylcellulose) or test compounds were orally administered once daily for 28 days. The vehicle was also given to C57BL/6J mice orally once daily for 28 days.

1.2.6. Analysis of Blood Glucose, Glucose Intolerance, and Plasma Parameter

I obtained whole blood samples (approximately 5 μL) from the tail vein under postprandial conditions and measured blood glucose with an automatic glucometer (Precision Exceed; Abbott Diabetes Care Ltd., Alameda, CA) on day 27 before final dosing. On day 28, I determined fasting blood glucose levels and performed oral glucose tolerance test (OGTT) under 18-hour fasting conditions. Blood glucose concentrations were quantified before and after glucose loading (1.5 g/kg p.o.) at different time points (0, 30, 60, 90, 120, 150, and 180 minutes) by the aforementioned method. On day 28, for plasma sampling, I also placed the mice under isoflurane anesthesia and collected whole blood from the inferior vena cava under postprandial conditions. Plasma samples

were obtained by centrifugation at 3,000 rpm at 4°C for 10 minutes. Plasma insulin and nonesterified fatty acid levels were determined by enzyme-linked immunosorbent assay (Shibayagi, Gunnma, Japan) and the colorimetric method (Wako Pure Chemical Industries, Osaka, Japan).

1.2.7. mtDNA Determination by Quantitative Real-Time PCR

I sacrificed vehicle or test compound-treated mice on day 28 by bleeding under anesthesia, rapidly removed the skeletal muscle (soleus and gastrocnemius muscle), and immediately froze it with liquid nitrogen. I isolated total DNA from the skeletal muscle using the QIAamp DNA Mini Kit (QIAGEN, Valencia, CA). The mtDNA level was quantified using the TaqMan gene expression assay system (Applied Biosystems, Foster City, CA). The PCR reaction was carried out in a 20 μL volume containing 2×TaqMan Universal Master Mix (Applied Biosystems, Foster City, CA), PCR-grade water (Roche Diagnostic Japan, Tokyo, Japan), TaqMan probes for the D-loop and thymidine kinase 1 regions, and the total DNA sample. The TaqMan probe sequence is shown in Table 1-1. I conducted PCR amplification with 40 cycles of the program at 95°C for 20 seconds, 95°C for 3 seconds, and 60°C for 30 seconds. Each sample was assayed in duplicate and the fluorescence spectra were continuously monitored by the 7500 Fast Real-Time PCR system with Sequence Detection Software, version 1.4 (Applied Biosystems/Life Technologies, Carlsbad, CA). Data analysis was based on measurement of the cycle threshold (Ct). The mtDNA copy number was determined from the standard curve and normalized by division of the D-loop value by the thymidine kinase 1 value. The data were expressed as relative values against the mtDNA level in C57BL/6J mice and shown as mean ± S.E.M..

1.2.8. Isolation of the Mitochondrial Fractions

I obtained skeletal muscle from the sacrificed mice and homogenized it with homogenizing

buffer (0.2 mol/L sucrose, 0.13 mol/L NaCl, 1.0 mmol/L Tris-HCl, pH=7.4) on ice. The homogenized sample was centrifuged at 3,000 rpm for 10 minutes at 4°C and the supernatant was again centrifuged at 14,000 rpm for 10 minutes. The supernatant was removed and the pellet (*i.e.*, the mitochondrial fraction) was dissolved in 0.25 mol/L sucrose. The mitochondrial fraction was frozen and thawed twice to assess mitochondrial respiratory chain enzyme activity.

1.2.9. Measurement of Mitochondrial Respiratory chain Enzyme Activity

To evaluate the short-duration effect of the test compounds on mitochondrial function, I assessed respiratory chain enzyme activity of the skeletal muscle mitochondrial fraction in db/db mice. Moreover, the mitochondrial function of compound-treated db/db mice was used to evaluate the chronic effect of test compounds on mitochondrial function. The assay was conducted as described previously, with slight modifications (Spinazzi *et al*., 2012). The reaction was carried out in 200 μL volume and detected by a microplate reader (SpectraMax 190; Molecular Devices, Sunnyvale, CA). The test compounds or DMSO were directly added to the reaction buffer (final concentration of DMSO was 1%) to assess the short-duration effects of the test compounds. Mitochondrial complex specific inhibitor, rotenone, malonate, and KCN were used as the reference compounds. Citrate synthase activity was measured as follows. The mitochondrial fraction was incubated in buffer containing 0.1 mmol/L 5,5′-dithiobis (2-nitrobenzoic acid) and 0.3 mmol/L acetyl-CoA at 37°C for 5 minutes. The reaction was started by adding 0.5 mmol/L oxaloacetic acid, and then I monitored the increase in absorbance at 412 nm for 3 minutes. Complexes I+III and II+III activities were measured by reduction of oxidized cytochrome *c* at an absorbance of 550 nm. In complexes I+III activity, 50 mmol/L Tris-HCl, 1 mmol/L KCN, 0.1 mmol/L NADH, and 0.1 mmol/L oxidized cytochrome *c* were incubated at 37°C for 5 minutes. The reaction was started by adding the sample, and the absorbance was observed for 3 minutes. In complexes II+III activity, 5 mmol/L potassium

phosphate buffer, 2 mmol/L KCN, 10 mmol/L sodium succinate dibasic, and the sample were incubated at 37°C for 10 minutes. The reaction was started by adding 0.1 mmol/L oxidized cytochrome *c*, and the absorbance change was observed for 3 minutes. Complex IV activity was measured by oxidation of reduced cytochrome *c* in absorbance at 550 nm. Reduced cytochrome *c* was prepared as described previously (Spinazzi *et al*., 2012). I incubated 5 mmol/L potassium phosphate buffer and reduced cytochrome *c* at 37°C for 5 minutes. The reaction was started by adding the sample, and the absorbance change was observed for 3 minutes. The results of complexes I+III, II+III, and complex IV activities were normalized by citrate synthase activity. Because of the variability of citrate synthase activity in each sample, respiratory chain enzyme activities were also normalized to each protein concentration. Data were expressed as relative values against vehicle-treated C57BL/6J mice enzyme activities and shown as mean ± S.E.M..

1.2.10. Data and Statistical Analysis

All data were expressed as mean ± S.E.M.. I calculated the areas under the curves using the trapezoidal rule from the blood glucose in the OGTT in C57BL/6J or db/db mice. I performed the statistical analysis using one-way analysis of variance followed by Dunnett's multiple comparison in three groups. A P value of < 0.05 was considered statistically significant.

1.3. Results

1.3.1. TT01001 Did Not Activate PPARγ but Interacted with mitoNEET

To evaluate the pharmacological properties of TT01001, I first examined the PPARγ activation effect by the TR-FRET method. No change in TR-FRET emission signal of TT01001 was seen in the concentration range of 0.001-100 μmol/L. On the other hand, pioglitazone increased the TR-FRET emission signals in a concentration-dependent manner (Fig. 1-2A). Next, to evaluate the binding effect of TT01001 for mitoNEET, I assessed the effect of TT01001 on mitoNEET protein by the SPR method using the Biacore instrument. The injection of TT01001 onto immobilized mitoNEET increased the RU in a concentration-dependent manner (1, 2, 4, 8, and 20 μmol/L) (Fig. 1-2B). Pioglitazone also increased the RU in a concentration-dependent manner (0.3, 0.6, 1.2, 2.5, and 5.0 μmol/L) (Fig. 1-2C).

1.3.2. TT01001 Improved Diabetes in db/db Mice without Causing Weight Gain

I next evaluated whether TT01001 could exhibit an ameliorative effect on glycemic parameters *in vivo*. I orally administered either TT01001 (100 mg/kg) or pioglitazone (30 mg/kg) to a genetically obese rodent model, db/db mice, once daily for 28 days. There was no effect of TT01001 on body weight, but it was increased by pioglitazone in a duration-dependent manner (Fig. 1-3A). On day 24, there were no body weight changes in TT01001-treated db/db mice; meanwhile, there was a significant increase in body weight in pioglitazone-treated db/db mice compared with vehicle-treated db/db mice (Fig. 1-3B). As for glycemic parameters, TT01001 treatment significantly decreased blood glucose levels (postprandial and fasting) (Fig. 1-3C and D). During the OGTT, blood glucose levels were lower in TT01001-treated db/db mice than in vehicle-treated db/db mice at all measurement points (Fig. 1-3E). Glucose areas under the curve (AUC 0-180 minutes in OGTT) were significantly decreased in TT01001-treated db/db mice (Fig. 1-3F). In the

plasma parameters of vehicle-treated db/db mice, a significant decrease was seen in the relative value of the endpoint of insulin concentration against the beginning of dosage compared with C57BL/6J mice. Neither TT01001 nor pioglitazone affected the plasma insulin levels (Fig. 1-3G). With regard to dyslipidemia, vehicle-treated db/db mice exhibited hyperlipidemia compared with C57BL/6J mice. There were significantly lower plasma nonesterified fatty acid levels in TT01001-treated db/db mice, similar to the changes seen with pioglitazone (Fig.1-3H).

1.3.3. Effect of TT01001 on mtDNA Levels and Mitochondrial Respiratory Chain Enzyme Activity

To reveal the effect of TT01001 on mitochondrial function, I examined the effects on mtDNA levels and mitochondrial respiratory chain enzyme activity in the skeletal muscle. The mtDNA level was significantly decreased in vehicle-treated db/db mice compared with that in C57BL/6J mice. Meanwhile, there were no differences in the mtDNA level of TT01001-or pioglitazone-treated db/db mice (Fig. 1-4). In addition to analyzing the mtDNA levels, I examined mitochondrial chain enzyme activity, and complexes I+III, II+III, and complex IV activity in db/db mice. First, I examined the short-duration effect of the test compounds on the mitochondrial respiratory chain enzyme activity of the skeletal muscle in db/db mice. There were no alterations in complexes I+II, II+III, and complex IV activities with either TT01001 or pioglitazone (10 or 30 μmol/L, respectively) (Fig. 1-5A-C). I next examined the chronic effects of the test compounds on mitochondrial respiratory chain enzyme activity in the skeletal muscle of db/db mice. There was no change in complexes I+III or complex IV activity of vehicle-or test compound-treated db/db mice compared with C57BL/6J mice (Fig. 1-6A and C). Meanwhile, complexes II+III activity was approximately 2-fold higher in vehicle-treated db/db mice than in C57BL/6J mice (Fig. 1-6B). We found that TT01001 significantly decreased complexes II+III activity compared with that in

vehicle-treated mice.

1.4. Discussion

The mitochondrial outer membrane protein mitoNEET, a binding protein of the insulin sensitizer pioglitazone, is considered a novel drug target for the treatment of type 2 diabetes (Colca *et al*., 2004). Kushiminski *et al*., demonstrated that the overexpression of mitoNEET in adipose tissues improved glycemic parameters, altered mitochondrial function, and decreased β-oxidation or membrane potentials (Kusminski *et al*., 2012). That report suggested an *in vivo* physiologic role of mitoNEET in glucose metabolism or mitochondrial function. On the other hand, although targeting mitoNEET is considered a novel strategy for the treatment of type 2 diabetes; there were no reports on the mitoNEET ligand effect on diabetes or mitochondrial function using animal disease models. In this study, I demonstrated the first experimental observation of the effects of the mitoNEET ligand on diabetes and mitochondrial function in type 2 diabetic model db/db mice.

Recently, TT01001 was synthesized as a new small-molecule compound on the basis of the pioglitazone structure. Pioglitazone has been known as a PPARγ agonist (Lehmann *et al*., 1995), thus I first examined the PPARγ activation effect of TT01001. TT01001 did not change TR-FRET emission signal; meanwhile, pioglitazone showed the increase of TR-FRET emission signal in a concentration-dependent manner. These results suggest that TT01001 did not show the activation effect of PPARγ. I next assessed the binding effect of TT01001 to mitoNEET by using recombinant mitoNEET and the SPR method. TT01001 increased the RU in a concentration-dependent manner, similar to pioglitazone on the immobilized recombinant mitoNEET. Previously, the binding effect of pioglitazone to mitoNEET was observed using liver mitochondrial suspension (Geldenhuys *et al*., 2010). Therefore, my SPR data suggest that TT01001 has a binding effect on mitoNEET. Collectively, TT01001 has *in vitro* pharmacological characteristics similar to the mitoNEET binding

effect, but not a PPARγ activation effect. To clarify whether oral administration of TT01001 could exhibit an ameliorative effect on diabetes, I examined the effects of TT01001 on glycemic parameters in db/db mice. Oral administration of TT01001 for 28 days significantly reduced blood glucose levels (postprandial and fasting) and improved glucose intolerance and hyperlipidemia, but not plasma insulin levels. These effects of TT01001 were almost equivalent to those of pioglitazone, indicating that TT01001 has a potent antidiabetic effect. Pioglitazone improves hyperglycemia and hyperlipidemia of db/db mice *via* an insulin-sensitizing effect on peripheral tissues (Suzuki *et al*., 2000). Thus, my data suggest that TT01001 improved peripheral glucose and lipid utilization in a manner similar to pioglitazone. In contrast to the apparent effects on glucose metabolism, pioglitazone significantly increased body weight in db/db mice. Weight gain is one of the major side effects of pioglitazone in clinical use (Gillies and Dunn, 2000), and it is attributed to pioglitazone's enhancement of PPARγ activation (Borsting *et al*., 2012). Therefore, weight gain in pioglitazone-treated db/db mice is considered a hallmark side effect of pioglitazone in clinical use. Interestingly, TT01001 has equivalent efficacy with pioglitazone on glycemic parameters, whereas it has no effect on body weight in db/db mice. As the possible reason for this phenomenon, although TT01001 bound to mitoNEET in a manner similar to pioglitazone, it did not exhibit the PPARγ activation effect. Taken together, TT01001 has therapeutic efficacy equivalent to the insulin-sensitizer pioglitazone without causing weight gain in db/db mice. Isolated heart mitochondria of mitoNEET-deficient mice show a decrease in state 3 respirations (Wiley *et al*., 2007). The overexpression of mitoNEET in genetic type 2 diabetic model ob/ob mice showed the alteration of mitochondrial functions (Kusminski *et al*., 2012). These reports may indicate that mitoNEET plays a physiologic role in mitochondrial function. To examine the effects of TT01001 on mitochondrial function, I first examined the effect of TT01001 on mitochondrial biogenesis in the skeletal muscle, which is a major target organ of insulin and plays an essential role in glucose

utilization (DeFronzo *et al*., 1979) in db/db mice. I observed significantly lower levels of mtDNA in vehicle-treated db/db mice compared with C57BL/6J mice. Since the mtDNA level is closely related to the pathology of type 2 diabetes (Lee *et al*., 1998; Song *et al*., 2001), decreased mtDNA levels in the skeletal muscle of vehicle-treated db/db mice were considered an alteration of mitochondrial function. However, I did not find that TT01001 and pioglitazone affected the mtDNA level in the skeletal muscle of db/db mice. A previous study showed that pioglitazone increased mtDNA copy numbers in the subcutaneous adipose tissue of patients with type 2 diabetes for 12 weeks after administration (Bogacka *et al*., 2005). Although the effects of TT01001 and pioglitazone on the mtDNA levels in adipose tissue are unknown, they may have no effect on the amount of mtDNA in skeletal muscle during an administration period of this length. Collectively, these data suggest that TT01001, at least in the skeletal muscle, did not have an effect on mitochondrial biogenesis. In the mitochondrial respiratory chain enzyme activity assay, TT01001 did not affect complexes I+III, II+III, or complex IV activity of the isolated mitochondrial fraction of the skeletal muscle from db/db mice during a short time period. On the other hand, in a chronic examination, TT01001 led to a significant reduction in the increase of complexes II+III activity without having an effect on complexes I+III or complex IV activity in the skeletal muscle of db/db mice. In db/db mice, mitochondrial respiration of the glycolytic skeletal muscle is enhanced under physiologic conditions (Holmström *et al*., 2012). Excess lipid increased the oxidative capacity and expression level of the mitochondrial respiratory chain subunit in the skeletal muscle of db/db mice (Turner *et al*., 2007). Possibly, as a result of enhanced complexes II+III activity in db/db mice this might indicate that it is a compensatory response to diabetic conditions, hyperglycemia, or hyperlipidemia. The skeletal muscle mitochondrial complex II has been reported to produce superoxide and/or hydrogen peroxide at relatively high rates (Quinlan *et al*., 2012). Accordingly, I speculate that compensatory enhanced complexes II+III activity leads to high production of superoxide and/or hydrogen peroxide, and they,

at least in part, contribute to type 2 diabetes conditions in db/db mice. It is possible that mitoNEET contributes to modulating oxidative stress *via* transferring iron into the mitochondrial matrix (Zuris *et al*., 2011). Therefore, mitoNEET may be a key regulatory protein of mitochondrial function, especially respiratory chain enzyme complex II or oxidative stress modulation. Possibly, TT01001 might ameliorate mitochondrial function toward normalization through the modulation of oxidative stress in the skeletal muscle of db/db mice. On the other hand, it was not clear how TT01001 suppressed the increase in complexes II+III activity with no effect on mitochondrial biogenesis or complexes I+III and complex IV activity. The practical concentration of TT01001 in target tissues and the binding affinity of it to mitoNEET have been unknown. Thus, a detailed analysis of mitoNEET on type 2 diabetes or mitochondrial function and pharmacokinetics-pharmacodynamics profiles of TT01001 is needed to elucidate the mechanism of action of TT01001. Further examination might identify the physiologic role of mitoNEET in type 2 diabetes or mitochondrial function.

1.5. Table

Table 1-1

TaqMan probes sequence for quantitative real time PCR

Primer sequence (5'→3')	D-loop	TK1
Forward	CCAAAAAACACTAAGAACTTGAAAGACA	GACTGTATTGAGCGGCTTCAGA
Probe	AATATTAACTATCAAACCCTATGTCC	TTCCCATGCTAAAACT
Revers	GTCATATTTTGGGAACTACTAGAATTGATC	CATGCTCGGTGTGAGCCATA

1.6. Figures

Figure 1-1

Chemical structures of TT01001 and pioglitazone

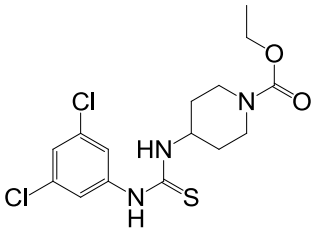

TT01001

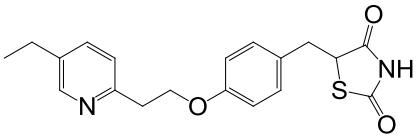

Pioglitazone

Figure 1-2

TT01001 did not activate PPARγ but interacted with mitoNEET.

The activity of PPARγ was assessed by the TR-FRET method using the LanthaScreen™ TR-FRET PPARγ coactivator assay kit (Invitrogen). TT01001 or pioglitazone (PIO) was incubated with the human PPARγ ligand-binding domain tagged with glutathione S-transferase, terbium-labeled anti–glutathione S-transferase antibody, and fluorescein peptide. Each line is expressed as a mean emission ratio of 520 and 495 nm (N = 4) in (A). The interaction of TT01001 and PIO was determined by the SPR method using Biacore S51. Different concentrations of TT01001 or PIO were injected onto the immobilized mitoNEET on a sensor chip (CM-5; GE Healthcare) for 60 seconds at a flow rate of 30 μl/min. Each line indicates the RU curves of (B) 1, 2, 4, 8, and 20 μmol/L TT01001 and (C) 0.3, 0.6, 1.2, 2.5, and 5.0 μmol/L, PIO, respectively.

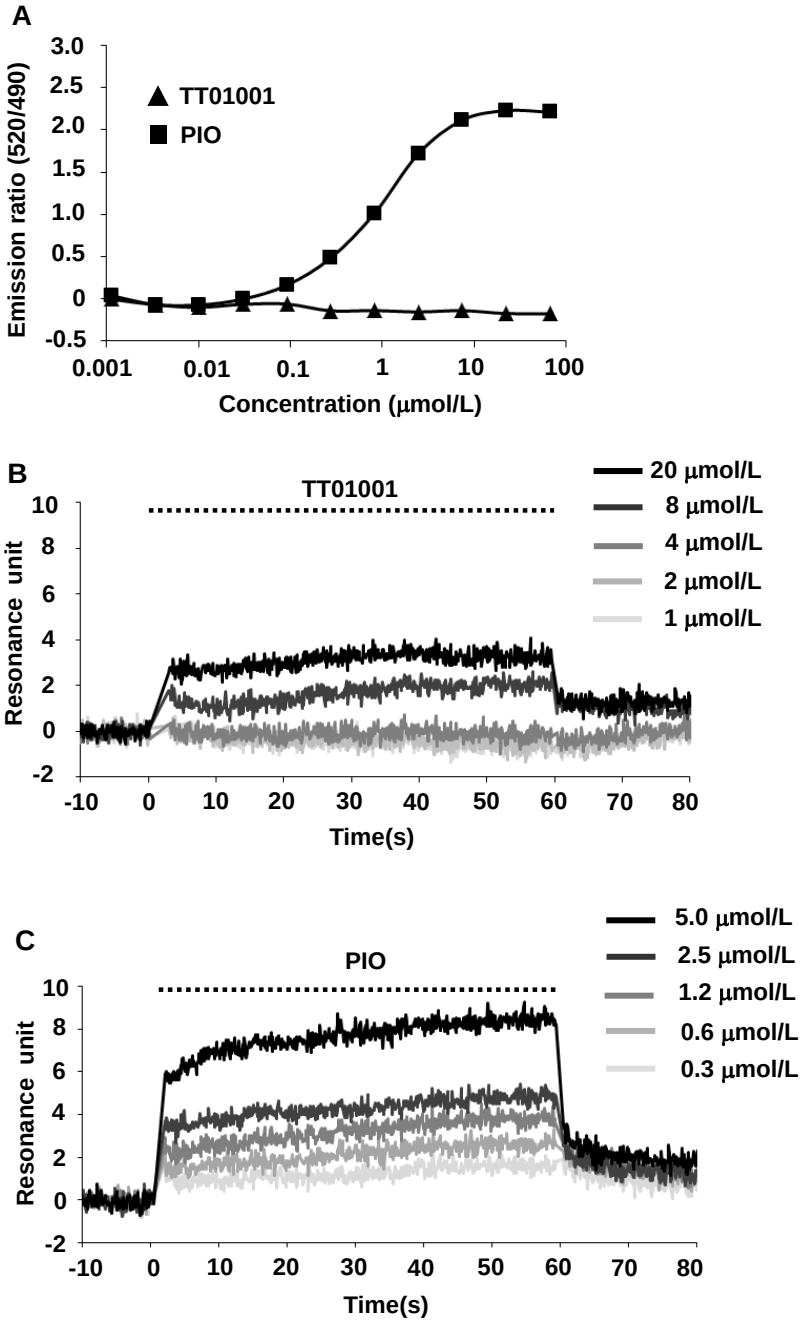
A
Emission ratio (520/490)
3.0
2.5
2.0
1.5
1.0
0.5
0
-0.5
TT01001
PIO
0.001
0.01
0.1
1
10
100
Concentration (μmol/L)
B
TT01001
Resonance unit
10
8
6
4
2
0
-2
20 μmol/L
8 μmol/L
4 μmol/L
2 μmol/L
1 μmol/L
-10
0
10
20
30
40
50
60
70
80
Time(s)
C
PIO
Resonance unit
10
8
6
4
2
0
-2
5.0 μmol/L
2.5 μmol/L
1.2 μmol/L
0.6 μmol/L
0.3 μmol/L
-10
0
10
20
30
40
50
60
70
80
Time(s)

Figure 1-3

TT01001 improved diabetes in db/db mice without causing weight gain

The vehicle (0.5% methylcellulose), TT01001 (100 mg/kg), or pioglitazone (PIO; 30 mg/kg) were orally administered to db/db mice once daily for 28 days. The vehicle was also orally administered to C57BL/6J mice. The courses of (A) body weight (N = 14), (B) body weight on day 24 (N = 14), (C) postprandial blood glucose levels (N = 14), (D) fasting blood glucose levels (N = 8), (E) blood glucose levels during the OGTT (N = 8), (F) blood glucose areas under the curves (0-180 minutes) (N = 8), (G) ratio of plasma insulin concentration between the beginning of dosage and end of dosage (N = 6), and (H) plasma concentration of nonesterified fatty acid (N = 6) are shown as means ± S.E.M.. *P<0.05; **P<0.01 compared with the vehicle-treated db/db mice by Dunnett's multiple test.

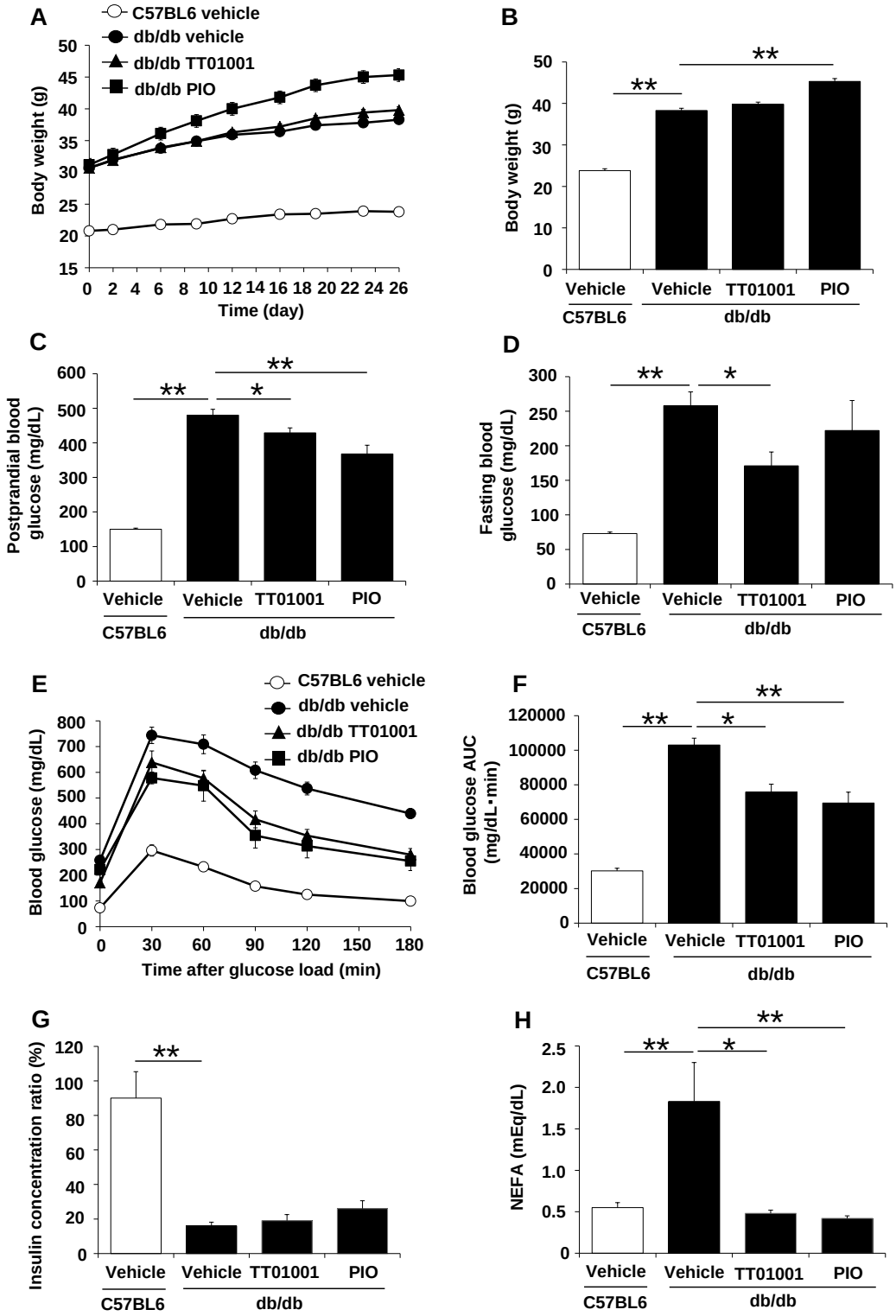
A
C57BL6 vehicle
db/db vehicle
db/db TT01001
db/db PIO
Body weight (g)
Time (day)
B
Body weight (g)
Vehicle
Vehicle
TT01001
PIO
C57BL6
db/db
C
Postprandial blood glucose (mg/dL)
D
Fasting blood glucose (mg/dL)
E
Blood glucose (mg/dL)
Time after glucose load (min)
F
Blood glucose AUC (mg/dL·min)
G
Insulin concentration ratio (%)
H
NEFA (mEq/dL)

Figure 1-4

TT01001 and pioglitazone (PIO) did not affect the mtDNA level in the skeletal muscle of db/db mice.

The vehicle (0.5% methylcellulose), TT01001 (100 mg/kg), or PIO (30 mg/kg) was orally administered to db/db mice once daily for 28 days. The vehicle was also orally administered to C57BL/6J mice. The mtDNA levels were determined by quantitative realtime PCR. Data are shown as means of the mtDNA ratio against C57BL/6J mice ± S.E.M.. $^{**}P < 0.01$ compared with the vehicle-treated db/db mice by Dunnett's multiple test ($N = 6$ animals per group).

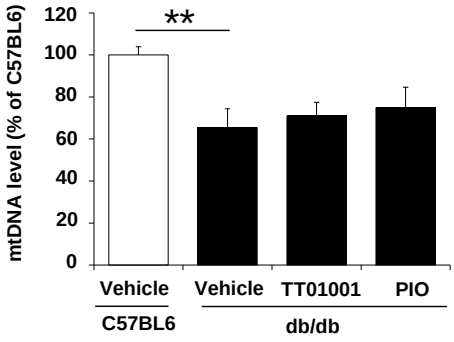
mtDNA level (% of C57BL6)
120
100
80
60
40
20
0
**
Vehicle
Vehicle
TT01001
PIO
C57BL6
db/db

Figure 1-5

TT01001 and pioglitazone (PIO) did not affect mitochondrial respiratory chain enzyme activity during a short time period.

DMSO, TT01001, or PIO was applied to the skeletal muscle mitochondrial fraction of db/db mice, and mitochondrial respiratory chain enzyme activity was measured by complexes (A) I+III, (B) complexes II+III, and (C) complex IV activities. Complex activity was normalized by citrate synthase activity in each sample. Mitochondrial complex-specific inhibitor, rotenone, malonate, and KCN were used as the reference compounds. Each assay was performed in triplicate and the data are shown as the means of ratios against the control (DMSO treatment) ± S.E.M.. Incubation times of TT01001 and PIO are 5 minutes for the complexes I+III and complex IV activity assays and 10 minutes for the complexes II+III activity assay, respectively.

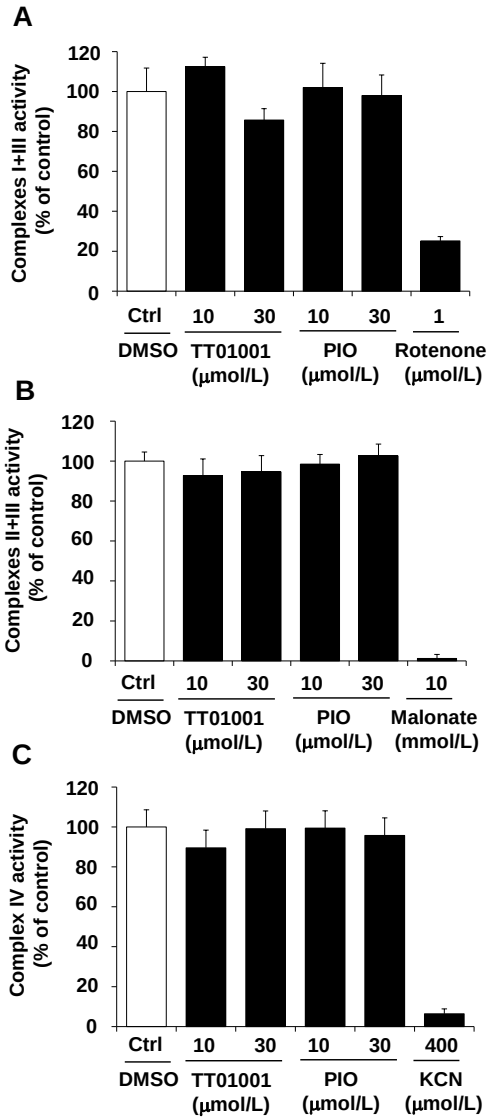
A
Complexes I+III activity (% of control)
120
100
80
60
40
20
0
Ctrl
10
30
10
30
1
DMSO
TT01001 (μmol/L)
PIO (μmol/L)
Rotenone (μmol/L)
B
Complexes II+III activity (% of control)
120
100
80
60
40
20
0
Ctrl
10
30
10
30
10
DMSO
TT01001 (μmol/L)
PIO (μmol/L)
Malonate (mmol/L)
C
Complex IV activity (% of control)
120
100
80
60
40
20
0
Ctrl
10
30
10
30
400
DMSO
TT01001 (μmol/L)
PIO (μmol/L)
KCN (μmol/L)

Figure 1-6

TT01001 decreased elevated complexes II+III activity in db/db mice

The vehicle (0.5% methylcellulose), TT01001 (100 mg/kg), or pioglitazone (PIO; 30 mg/kg) was orally administered to db/db mice once daily for 28 days. The vehicle was also orally administered to C57BL/6J mice. The mitochondrial fraction was isolated from vehicle- or compound-treated mice, and mitochondrial respiratory chain enzyme activity was measured by (A) complexes I+III, (B) complexes II+III, and (C) complex IV activities. The data are shown as the means of ratios against vehicle-treated C57BL/6J mice ± S.E.M.. **P*<0.05, ***P*<0.01 compared with the vehicle-treated db/db mice by Dunnett's multiple test (*N* = 6 animals per group).

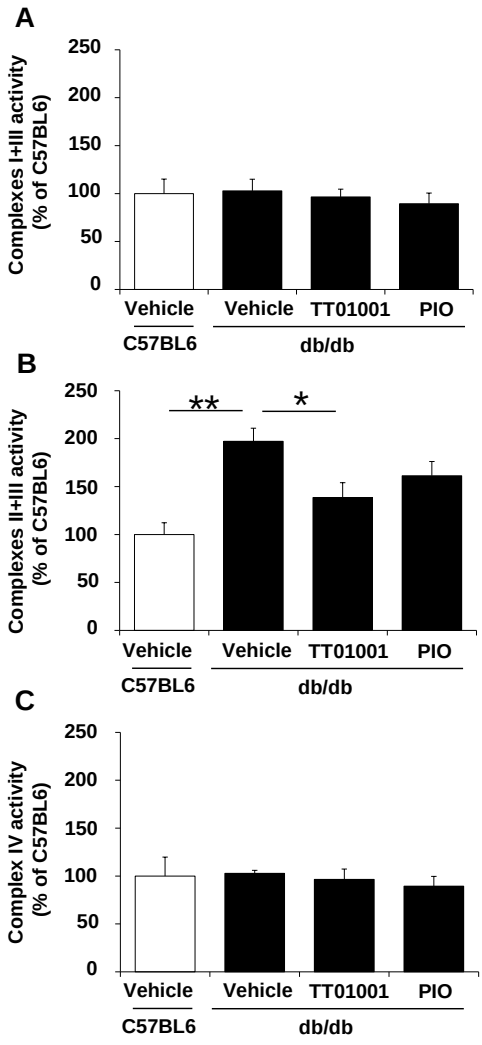
A
Complexes I+III activity (% of C57BL6)
250
200
150
100
50
0
Vehicle
Vehicle
TT01001
PIO
C57BL6
db/db
B
Complexes II+III activity (% of C57BL6)
**
*
250
200
150
100
50
0
Vehicle
Vehicle
TT01001
PIO
C57BL6
db/db
C
Complex IV activity (% of C57BL6)
250
200
150
100
50
0
Vehicle
Vehicle
TT01001
PIO
C57BL6
db/db

Chapter 2: Pharmacological properties of HIS-388, a novel 11β-HSD1 inhibitor

2.1. Introduction

11β-Hydroxysteroid dehydrogenase type 1 (11β-HSD1) is a key enzyme that catalyzes the conversion of the active glucocorticoid cortisol from its inactive metabolite cortisone (Harno and White, 2010). 11β-HSD1 is abundant in the liver and adipose tissue, and higher adipose 11β-HSD1 activity is associated with features of the metabolic syndrome (Lindsay *et al*., 2003). 11β-HSD1 deficient mice have normal or minimally increased plasma glucocorticoid levels but cannot regenerate glucocorticoid within cells in the liver and adipose tissue. As a result, they are protected against insulin resistance, hyperglycemia, and weight gain induced by a high-fat diet (Kotelevtsev *et al*., 1997). Conversely, mice overexpressing 11β-HSD1 in adipose tissue have increased intra-adipose glucocorticoid concentrations despite unchanged plasma levels. These mice show remarkable features of the metabolic syndrome, such as obesity, insulin resistance, glucose intolerance, and hyperglycemia (Masuzaki *et al*., 2001, 2003; Paterson *et al*., 2004). These findings suggest that 11β-HSD1 is a potential therapeutic target for the treatment of type 2 diabetes. Many selective 11β-HSD1 inhibitors have been explored as a new approach for the treatment of type 2 diabetes. In fact, several 11β-HSD1 inhibitors, such as compound 544 (Cpd544), BVT2733, and KR-66344 improve insulin sensitivity or glucose intolerance in some animal models (Alberts *et al*., 2003; Hermanowski-Vosatka *et al*., 2005; Park *et al*., 2011). Although BVT116429 shows a high potency for 11β-HSD1 inhibition *in vitro*, it has no effect on glucose intolerance in type 2 diabetic mice (Sundbom *et al*., 2008). Thus, although compounds show a high potency for 11β-HSD1 inhibition *in vitro*, it is unclear whether these compounds have an equivalent effect on insulin resistance or glucose intolerance *in vivo*. Recently, HIS-388 was synthesized as a novel 11β-HSD1 inhibitor. In this study, I investigated the pharmacological properties of HIS-388 in several animal

models. In chapter 2, first, I assessed the effect of HIS-388 on *in vivo* 11β-HSD1 enzyme activity in mice with cortisone-induced hypercortisolism and hyperinsulinemia. Furthermore, I explored whether HIS-388 can improve insulin sensitivity and glucose intolerance in two different animal models, namely mice with high fat diet-induced obesity (DIO) or the non-genetic type 2 diabetes murine model, with the latter produced by the combination of a high-fat diet (HFD) and low doses of streptozotocin (HFD/STZ mice).

2.2. Materials & Methods

2.2.1. Chemicals

HIS-388 (Fig. 2-1) and Cpd544 were synthesized in the Pharmaceutical Laboratories of Toray Industries, Inc. (Kanagawa, Japan). Carbenoxolone (CBX), pioglitazone hydrochloride, and 21-day slow-release cortisone pellet were purchased from Sigma-Aldrich Japan (Tokyo, Japan), Kemprotec Limited (Middlesbrough, UK), and Innovative Research of America (Sarasota, FL), respectively. Other chemicals were purchased from Sigma-Aldrich Japan. In the enzyme assay, HIS-388, CBX, and Cpd544 were dissolved in DMSO. For *in vivo* experiments, HIS-388, CBX, Cpd544, and pioglitazone were suspended in 0.5% methylcellulose. To prepare the non-genetic type 2 diabetes animal model involving HFD/STZ mice, streptozotocin (STZ) was dissolved in saline.

2.2.2. *In vitro* Enzyme Assay

The 11β-HSD1 enzyme assay was carried out using human and mouse liver microsomes (MS). Human MS (mixed sex) was purchased from XenoTech (Lenexa, KC). The MS protein (50 μg/ml), substrate cortisone (160 nmol/L), and nicotinamide adenine dinucleotide phosphate (NADPH) (200 nmol/L) were added to an assay buffer (20 mmol/L HEPES with 5 mmol/L EDTA, pH 6.0) with or without 11β-HSD1 inhibitors (HIS-388, CBX or Cpd 544) and incubated for 2 hours at 37°C. The amount of cortisol in the reaction mixture was measured by homogenous time-resolved fluorescence (HTRF) assay system (Cisbio, Bedford, MA). Mouse MS was prepared according to a method described previously (Kushiro *et al*., 2004). The MS protein (10 μg/ml) from ICR mouse liver, substrate 11-dehydrocorticosterone (20 nmol/L) obtained from Innovative Research of America, and NADPH (200 μmol/L) were added to the assay buffer and incubated for 2 hours at 37°C. The amount of corticosterone in the reaction mixture was measured by enzyme-linked immunosorbent assay (ELISA) (Cayman Chemical, Ann Arbor, MI). The percentage inhibition was

calculated and plotted against test compound concentration to generate the IC_{50}.

2.2.3. Animals

This study was reviewed by the Animal Care and Use Committee and approved by the head of the test facility and performed in accordance with the Guideline for Animal Experiments, Research and Development Division, Toray Industries, Inc. All mice were purchased from Charles River Laboratories Japan Inc. (Kanagawa, Japan) and group-housed in cages at a temperature of 22-24°C with a 12-hour light/dark cycle (lights on at 7:00 AM) for at least 1 week before experiments. Mice were given access to food and water *ad libitum*.

2.2.4. Cortisone-Implanted Mice

Ten-week-old male C57BL/6J mice were anesthetized with pentobarbital sodium (70 mg/kg i.p.). The back skin of the neck was cut open, and a subcutaneous longitudinal pocket was created about 3 cm beyond the incision site toward the lower back. A cortisone pellet (1.5 or 35 mg) was implanted, and the incision site was closed using wound glue. Sham-operated mice did not have cortisone pellet implants. After more than 3 days of recovery from surgery, single doses of HIS-388, CBX, and Cpd544 were orally administered at a dose of 30 mg/kg in cortisone pellet (35 mg)-implanted mice to investigate the ability of compounds to inhibit *in vivo* 11β-HSD1 enzyme activity. Whole blood was sampled from the tail vein before and after administration of compounds at different time points (0, 1, 4, 8, and 24 hours). Plasma cortisol and insulin levels were quantified at all-time points and 24 hours after administration of compounds, respectively.

2.2.5. Mice with diet-induced obesity (DIO mice)

Four-week-old male C57BL/6J mice were given regular chow (CRF-1; Oriental Yeast Co.,

Tokyo, Japan) or a HFD (D12492; Research Diets, Inc., New Brunswick, NJ) for 12-13 weeks. To evaluate the efficacy of HIS-388 (30 mg/kg, 100 mg/kg) against insulin resistance and obesity, mice were weighed regularly to allow accurate HIS-388 dosing, which was orally administered once daily for 14 days (days 0-13). After the final dosing of HIS-388, mice were deprived of food for 18 hours. Blood glucose concentration was then measured, and whole blood was sampled *via* the tail tip. To compare the efficacy of HIS-388 (30 mg/kg) and pioglitazone (30 mg/kg) in DIO mice, these compounds were orally administered once daily for 14 days (days 0-13). After the final administration, blood glucose level was determined, and whole blood was collected under a fasting condition. The insulin tolerance test (ITT) was also performed under fasting conditions by intraperitoneal injection of regular human insulin (0.3 U/kg Humulin; Eli Lilly Japan, Kobe, Japan). The concentration of blood glucose was measured before and after insulin injection at different time points (30, 60, 90, and 120 minutes). To clarify the effect of HIS-388 on hepatic insulin resistance, the pyruvate tolerance test (PTT) was performed. Basal blood glucose level was determined, and 1.5 g/kg sodium pyruvate (dissolved in saline) was injected into the peritoneum of overnight-fasted mice. The concentration of blood glucose was measured at 30, 60, 90, 120, and 180 minutes after sodium pyruvate injection.

2.2.6. HFD/STZ, non-genetic type 2 diabetes mice

Non-genetic type 2 diabetes mice were prepared as described previously (Luo *et al*., 1998; Mu *et al*., 2009) with slight modifications. In brief, 5-week-old male C57BL/6J mice received regular chow (CRF-1; Oriental Yeast Co., Tokyo, Japan) or a HFD (D12492; Research Diets, Inc., New Brunswick, NJ) for 4 weeks to generate peripheral insulin resistance. The mice were given an intraperitoneal injection of STZ at 100 mg/kg and maintained for 14 days under the above condition. Control mice did not receive STZ administration or a HFD. HIS-388 (30 mg/kg) and

pioglitazone (30 mg/kg) were orally administered once daily for 15 days (days 0-14). On day 14, blood glucose concentration was determined, and blood samples were taken under feeding conditions. After the final administration of compounds, the OGTT was performed under an 18-hour fasting condition. Blood glucose concentration was quantified before and after glucose loading (1.5 g/kg) at different time points (0, 20, 40, 60, and 120 minutes) by following the above-mentioned method.

2.2.7. Measurement of Food Intake.

Four-week-old male C57BL/6J or 6N mice were treated with regular chow for 11 weeks (normal) or HFD for 40 weeks (DIO). These mice were used for the measurement of food intake. Vehicle or HIS-388 was orally administrated once daily for 7 days in normal mice (30 or 100 mg/kg) and for 12 days in DIO mice (30 mg/kg). Food intake was calculated as the difference between the food provided and the food remaining on an arbitrary day.

2.2.8. Blood Sample Assay

Blood glucose level was measured with an automatic glucometer (Precision Xceed; Abbott Diabetes Care Ltd., Alameda, CA). The plasma was obtained by centrifuge of collected whole blood samples. Plasma cortisol and insulin concentrations were quantified by the HTRF assay system (Cisbio, Bedford, MA) and ELISA (Shibayagi, Gunma, Japan), respectively.

2.2.9. Statistical Analysis

Data were expressed as mean or mean ± S.E.M.. Homeostasis model assessment-insulin resistance (HOMA-IR) score as an insulin resistance index was calculated according to the formula (Lee *et al*., 2002; Pickavance *et al*., 2005): fasting blood glucose (mg/dL) × fasting plasma insulin

(ng/mL)/22.5. Areas under the curves (AUCs) were calculated using trapezoidal rule from the blood glucose change in ITT, PTT, and OGTT in DIO or HFD/STZ mice and the temporal changes in plasma cortisol level in cortisone-implanted mice. Statistical analysis was performed using one-way analysis of variance followed by Dunnett's or Tukey's multiple comparison for three or more groups or using the t test for two groups. A P values of < 0.05 were considered statistically significant.

2.3. Results

2.3.1. *In Vitro* 11β-HSD1 Inhibitory Effect of HIS-388

I assessed the *in vitro* enzyme activity by HTRF or ELISA methods using human or mice liver MS. CBX and Cpd544 were used as reference compounds. HIS-388 displayed inhibitory effects on 11β-HSD1 enzyme activity, and the IC_{50} values were 14.7 and 82.0 nmol/L in human and mice, respectively. The inhibitory effects of HIS-388 and CBX on murine 11β-HSD1 enzyme activity were almost equivalent; however, Cpd544 had lower potency than HIS-388 (Table 2-1).

2.3.2. Effect of HIS-388 on *In Vivo* 11β-HSD1 Activity in Cortisone-Implanted Mice

To evaluate the efficacy of HIS-388 against *in vivo* 11β-HSD1 enzyme activity, I examined its effect on plasma cortisol and insulin concentration in slow release cortisone pellet-implanted mice. In cortisone-implanted mice, the plasma cortisol and insulin, but not glucose levels were increased in a cortisone dose-dependent manner, indicating that *in vivo* 11β-HSD1 enzyme activity contributes to this phenomenon (Fig. 2-2). Since the high-dose (35 mg) cortisone pellet strongly elevated plasma concentrations of cortisol and insulin, I adopted this dose for the following evaluation. I found a remarkable decrease of plasma cortisol concentration after HIS-388 administration. The efficacy of CBX was weaker than HIS-388 (Fig. 2-3A and B). Although Cpd544 reduced plasma cortisol concentration at 1 hour after administration, this effect rapidly disappeared 4 hours after administration (Fig. 2-3C and D). Moreover, HIS-388, but not CBX and Cpd544, decreased plasma insulin levels at 24 hours after administration (Fig. 2-3E and F), indicating that HIS-388 has a potent and continuous suppressive effect on 11β-HSD1 enzyme activity *in vivo*.

2.3.3. Effect of HIS-388 on Obesity and Insulin Resistance in DIO Mice

To test the effect of HIS-388 on obesity and insulin resistance, HIS-388 was given to DIO mice for 14 days. A significant decrease in body weight was observed in HIS-388-treated DIO mice in a dose-dependent fashion (Fig. 2-4A). HIS-388 also significantly reduced fasting blood glucose levels at a high dose (100 mg/kg) (Fig. 2-4B). Moreover, fasting plasma insulin levels and HOMA-IR score in HIS-388-treated DIO mice were significantly lower in a dose-dependent manner compared with vehicle-treated mice (Fig. 2-4C and D).

2.3.4. Effect of HIS-388 on Food Intake

In normal mice, there were no differences in food intake and body weight after HIS-388 (30 and 100 mg/kg) treatment (Fig. 2-5A and B). In DIO mice, food intake remarkably decreased on day 2 after HIS-388 (30 mg/kg) administration. From day 2 onward, slight reduction was observed on days 7 and 12 compared with vehicle-treated mice (Fig. 2-5C). Weight reduction was observed in HIS-388-treated DIO mice, followed by a decrease in food intake (Fig. 2-5D).

2.3.5. Comparative Study of the Therapeutic Efficacy of HIS-388 and Pioglitazone against Insulin Resistance in DIO Mice

Because the inhibition of 11β-HSD1 by HIS-388 ameliorated obesity and insulin resistance in DIO mice (Fig. 2-4), I conducted a comparative study of the therapeutic efficacy of HIS-388 (30 mg/kg per day) and pioglitazone (30 mg/kg per day) against insulin resistance in DIO mice. A significant decrease in body weight was observed in DIO mice treated with HIS-388, as shown above. Meanwhile, pioglitazone treatment slightly increased body weight (Fig. 2-6A). Fasting blood glucose, insulin levels, and HOMA-IR score were significantly decreased in HIS-388-treated DIO mice, the results of which were indistinguishable from those of pioglitazone treatment (Fig. 2-6B-D). HIS-388 ameliorated insulin sensitivity to the same degree as pioglitazone in ITT (Fig.

2-6E and F). Furthermore, I carried out the PTT in DIO mice to estimate the site of action of HIS-388 in the liver. During the PTT, blood glucose levels of HIS-388-treated DIO mice were lowered, and the AUC was significantly decreased compared with those of vehicle-treated DIO mice (Fig. 2-6G and H).

2.3.6. Comparative Study of the Therapeutic Efficacy of HIS-388 and Pioglitazone against Glucose Intolerance in HFD/STZ, Non-genetic Type 2 Diabetes Mice

I next examined the therapeutic efficacy of HIS-388 compared with pioglitazone in the non-genetic type 2 diabetes model involving HFD/STZ mice, which is produced by combined HFD feeding and STZ injection. Injection of 100 mg/kg STZ did not affect postprandial blood glucose and plasma insulin levels. In mice treated with HFD, postprandial plasma insulin, but not blood glucose level, was significantly increased compared with those in control mice (Fig. 2-7A and B). Furthermore, an increase in the postprandial blood glucose level and a decrease of the postprandial plasma insulin level were observed in HFD/STZ (vehicle treatment) mice compared with those in mice that were fed a HFD (Fig. 2-7A and B). During OGTT, blood glucose levels and glucose AUC were significantly increased in HFD/STZ (vehicle treatment) mice, although no significant changes were seen in mice treated with STZ or HFD compared with control mice (Fig. 2-7C and D). These results indicated that combined HFD and STZ injection produced mild hyperglycemia, mild hyperinsulinemia, and glucose intolerance, and HIS-388 decreased postprandial blood glucose and insulin levels in HFD/STZ mice (Fig. 2-7A and B). In addition to these effects, HIS-388 significantly decreased blood glucose AUC in the OGTT compared with that in vehicle-treated mice. The effects on glucose intolerance in HIS-388-treated HFD/STZ mice were indistinguishable from those in pioglitazone-treated mice, indicating that HIS-388 has a similar efficacy to pioglitazone in this murine model (Fig. 2-7C and D).

2.4. Discussion

It has been reported that the small molecule 11β-HSD1 inhibitor ameliorated insulin sensitivity or glucose intolerance in rodent models related to diabetes or obesity (Anagnostis *et al*., 2013). For instance, Cpd544 ameliorated insulin sensitivity and hyperglycemia and reduced body weight with improvement of the lipid profile in DIO mice (Hermanowski-Vosatka *et al*., 2005). BVT2733 increased insulin sensitivity and decreased endogenous glucose production under a euglycemic, hyperinsulinemic state in KKAy mice (Alberts *et al*., 2003). KR-66344 also improved glucose intolerance and suppressed adipocyte differentiation in ob/ob mice (Park *et al*., 2011). Although BVT116429 has selective and potent 11β-HSD1 inhibitory effect *in vitro*, BVT116429 had no effect on glucose intolerance in type 2 diabetic mice (Sundbom *et al*., 2008). Therefore, in addition to *in vitro* 11β-HSD1 inhibitory activity, another pharmacological property may be involved in the improvement of glucose intolerance or insulin resistance. In the present study, I demonstrated that HIS-388, a novel 11β-HSD1 inhibitor that exhibits potent and long-acting suppression of *in vivo* 11β-HSD1 enzyme activity, has therapeutic efficacy against insulin resistance and glucose intolerance indistinguishable from those of a potent insulin sensitizer, pioglitazone, in DIO mice and non-genetic type 2 diabetes mice. I examined the effect of HIS-388, which inhibits 11β-HSD1 enzyme activity with a potency equivalent to that of CBX but greater than that of Cpd544 *in vitro*, on *in vivo* 11β-HSD1 enzyme activity using the cortisone pellet implant murine model. This model shows an increase of plasma cortisol and insulin levels. These alterations are attributed to the conversion of inactive cortisone to active cortisol *via* an *in vivo* 11β-HSD1 enzyme reaction (Bhat *et al*., 2008). In the present study, plasma cortisol and insulin levels were increased in a dose-dependent manner in mice with cortisone pellet implants. These results were consistent with those of a previous report; therefore, I applied this animal model to the evaluation of *in vivo* 11β-HSD1 enzyme activity, including the evaluation of potency and long-acting effects. Single dosing of HIS-388 suppressed the

increase of plasma cortisol level in this model. The suppressive effect of HIS-388 on plasma cortisol level was more potent or longer than those of CBX or Cpd544. Moreover, HIS-388, but not CBX or Cpd544, decreased plasma insulin levels. These data suggest that HIS-388 has a potent and long-acting inhibitory effect on 11β-HSD1 enzyme activity *in vivo*. To assess the effect of HIS-388 on obesity and insulin resistance, I next examined the efficacy of HIS-388 (30 and 100 mg/kg) in DIO mice. HIS-388 reduced body weight in a dose-dependent manner in DIO mice, which suggests a potent antiobesity effect. This weight reduction was not observed in normal C57BL/6J mice treated with HIS-388 (30 and 100 mg/kg) (Fig. 5A). These data indicated that the weight reduction effect of HIS-388 is a characteristic phenomenon in DIO and possibly other disease model mice. In general, food intake is closely related to body weight change. Some 11β-HSD1 inhibitors exhibit reduction of food intake in DIO mice (Hermanowski-Vosatka *et al*., 2005; Wang *et al*., 2006). In contrast, overexpression of 11β-HSD1 in adipose tissue is associated with increased food intake (Masuzaki *et al*., 2001). These reports indicate that 11β-HSD1 activity is involved in food intake regulation. HIS-388 decreased food intake in DIO mice but not in normal mice (Fig. 5A and C), indicating that these data are consistent with the results of the previous report. Therefore, this effect, at least in part, may be involved in the decrease of weight reduction in DIO mice. HIS-388 dose-dependently decreased blood glucose and plasma insulin levels in the fasting state and HOMA-IR score in DIO mice. In preliminary study, I found that single administration of HIS-388 dose-dependently inhibited 11β-HSD1 enzyme activity; however, it is not completely inhibited at the dose of 30 mg/kg 6 hours after administration in pioglitazone-treated DIO mice. This weight gain was considered to be an adverse side effect of pioglitazone that is seen in clinical practice (Gillies and Dunn, 2000). As for insulin resistance, HIS-388 ameliorated parameters of insulin resistance such as blood glucose, plasma insulin levels in the fasting state, and the HOMA-IR score and enhanced insulin sensitivity to the same degree as that of pioglitazone. Glucocorticoids contribute to increased hepatic glucose

production in diabetes and counteract the actions of insulin (Friedman *et al*., 1993). Accordingly, 11β-HSD1-deficient mice or treatment with an 11β-HSD1 inhibitor in the type 2 diabetes model displayed amelioration of hepatic insulin resistance (Morton *et al*., 2001; Alberts *et al*., 2003). These reports imply that hepatic 11β-HSD1 activation leads to insulin resistance in the liver. Thus, to reveal the pharmacological characteristics of HIS-388, I performed the PTT in DIO mice. After pyruvate injection, blood glucose levels in HIS-388-treated DIO mice were lower than those in vehicle-treated mice. A significant decrease in blood glucose AUC was also observed in HIS-388-treated DIO mice. Taken together, these results suggest that the ameliorative effect of HIS-388 on insulin resistance is comparable to that of pioglitazone in DIO mice. Moreover, it is considered that the insulin sensitizing effects of HIS-388 may be at least in part due to its antiobesity effect and improvement of hepatic insulin resistance *via* inhibition of 11β-HSD1 enzyme activity in DIO mice. Combined HFD and low-dose STZ elicited mild hyperglycemia, insulin deficiency, and reduction of glucose uptake in rodents, which partly mimic human type 2 diabetes. Thus, HFD/STZ mice are regarded as a non-genetic type 2 diabetes model (Mu *et al*., 2009). To further evaluate the therapeutic effect of HIS-388 from the point of glucose control, I compared the effect of HIS-388 with pioglitazone on glucose intolerance in HFD/STZ mice. HIS-388 reduced postprandial blood glucose and plasma insulin levels and improved glucose intolerance. These effects of HIS-388 were indistinguishable from those of pioglitazone treatment, indicating that HIS-388 may have a therapeutic efficacy against glucose intolerance that is almost equal to that of pioglitazone in the non-genetic type 2 diabetes model. The effects of HIS-388 on biochemical parameters, postprandial blood glucose, and insulin levels was observed to the same degree as those of the potent insulin sensitizer pioglitazone, thus suggesting that its mechanism of action might be through improved insulin sensitivity. Cpd544 decreased blood glucose levels (postprandial and fasting), increased insulin sensitivity, and improved glucose intolerance in HFD/STZ mice by twice daily administration (Hermanowski-Vosatka *et al*.,

2005). By focusing on the administration frequency in this animal model, pharmacological efficacy of HIS-388 could be achieved by once daily administration. These results suggest that potent and long-acting inhibition of 11β-HSD1 may contribute to the efficacy on insulin sensitivity and glucose intolerance in HFD/STZ mice.

2.5. Table

Table 2-1

***In vitro* 11β-HSD1 inhibitory activity of HIS-388**

Potency of test substance against human (h) and mouse (m) 11β-HSD1 was determined using liver microsomes and expressed as IC_{50}. The values are means of at least two determinations.

Compound	Liver MS IC_{50} (nmol/L)	
	hHSD1	mHSD1
HIS-388	14.7	82.0
CBX	550	115
Cpd544	20.9	269

2.6. Figures

Figure 2-1

Chemical structure of HIS-388

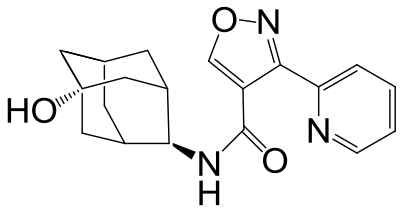

HIS-388

Figure 2-2

Effect of cortisone pellet implantation on metabolic parameters in mice.

A 21-day slow-release cortisone pellet (1.5 or 35 mg per pellet) was implanted into the subcutaneous tissue of mice. After recovery from surgery, blood was sampled from the tail vein for assessment of metabolic parameters. Plasma cortisol (A), plasma insulin (B), and blood glucose (C) levels are shown. Values are means ± S.E.M.. $^{**}P<0.01$ compared with the sham-operated group by Dunnett's test. N = 4-10 animals per group. NS, not significant.

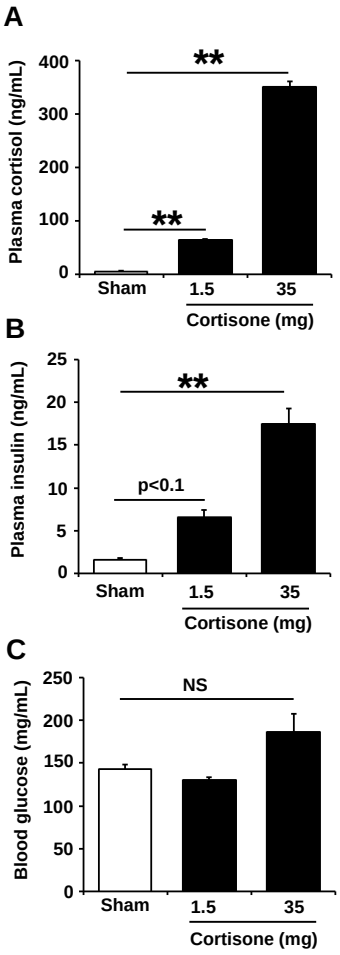
A
Plasma cortisol (ng/mL)
400
300
200
100
0
**
**
Sham
1.5
35
Cortisone (mg)
B
Plasma insulin (ng/mL)
25
20
15
10
5
0
**
p<0.1
Sham
1.5
35
Cortisone (mg)
C
Blood glucose (mg/mL)
250
200
150
100
50
0
NS
Sham
1.5
35
Cortisone (mg)

Figure 2-3

Effect of 11β-HSD1 inhibitors on plasma cortisol and insulin levels in cortisone pellet-implanted mice

Cortisone 35 mg pellets were implanted into the subcutaneous tissue of mice. After recovery from surgery, 30 mg/kg of HIS-388, CBX or Cpd544 were administered orally to mice, and blood samples were collected at 0, 1, 2, 4, 8, and 24 hours after administration. Time course of plasma cortisol levels (A and C), plasma cortisol AUC 0–8 hours (B and D), and change of plasma insulin levels (E and F) are shown. Cortisol and insulin levels at 0 hours were defined as baseline (100%), and values at other time points were calculated as percentage of baseline. Values are means ± S.E.M.. *P<0.05; 5. **P<0.01 compared with vehicle-treated group by Dunnett's test. N = 4-5 animals per group.

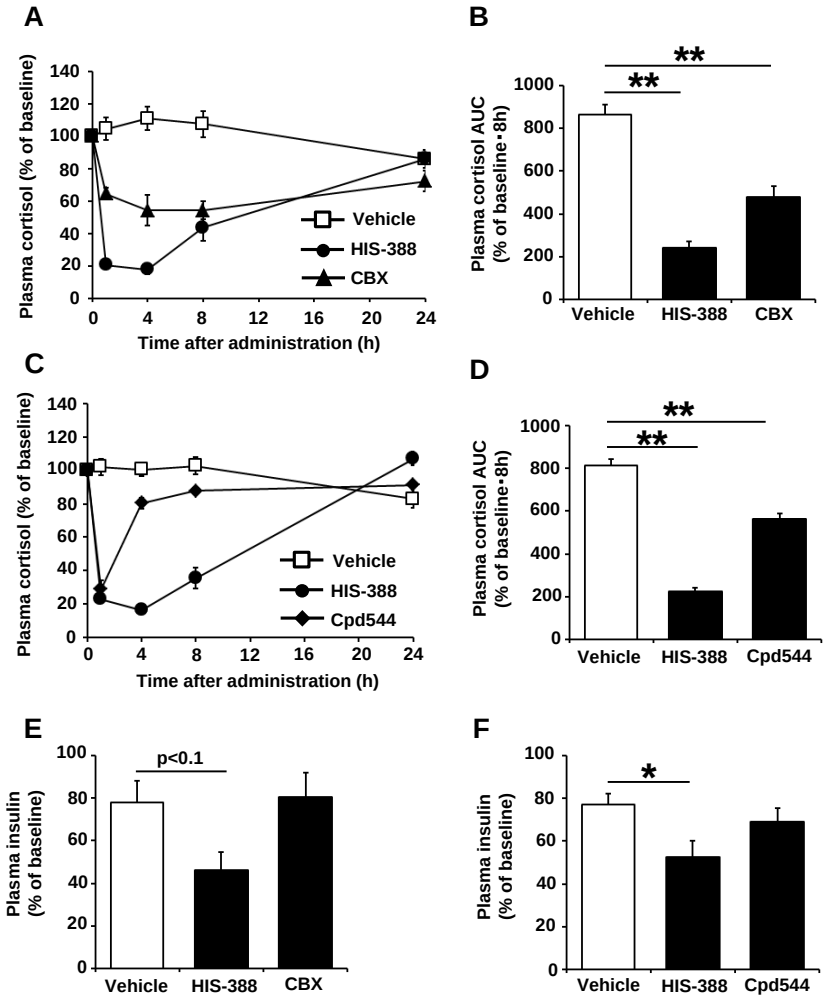
A
Plasma cortisol (% of baseline)
140
120
100
80
60
40
20
0
0
4
8
12
16
20
24
Time after administration (h)
Vehicle
HIS-388
CBX
B
Plasma cortisol AUC
(% of baseline•8h)
1000
800
600
400
200
0
**
**
Vehicle
HIS-388
CBX
C
Plasma cortisol (% of baseline)
Time after administration (h)
Vehicle
HIS-388
Cpd544
D
Plasma cortisol AUC
(% of baseline•8h)
**
**
Vehicle
HIS-388
Cpd544
E
Plasma insulin
(% of baseline)
p<0.1
Vehicle
HIS-388
CBX
F
Plasma insulin
(% of baseline)
*
Vehicle
HIS-388
Cpd544

Figure 2-4

Effects of HIS-388 on body weight and diabetic parameters, fasting blood glucose, plasma insulin levels, and HOMA-IR index

HIS-388 (30 and 100 mg/kg) was administered orally once daily for 14 days. After the final administration, mice were food deprived for 18 hours, and blood samples were collected for measurement of blood glucose and plasma insulin. Body weight (A), fasting blood glucose (B), fasting plasma insulin (C), and HOMA-IR (D) levels are shown. Values are means ± S.E.M.. *P<0.05; **P<0.01 compared with vehicle-treated group by Dunnett's test. N = 8 animals per group.

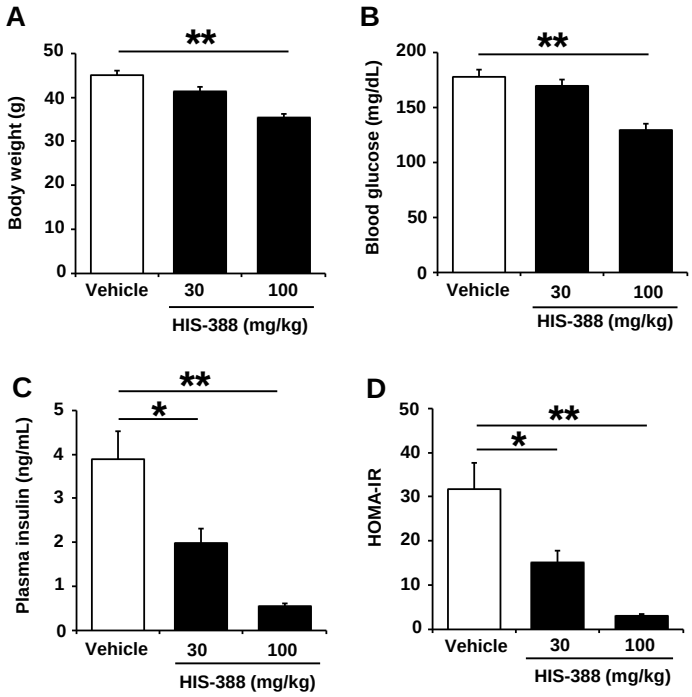
A
**
Body weight (g)
50
40
30
20
10
0
Vehicle
30
100
HIS-388 (mg/kg)
B
**
Blood glucose (mg/dL)
200
150
100
50
0
Vehicle
30
100
HIS-388 (mg/kg)
C
**
*
Plasma insulin (ng/mL)
5
4
3
2
1
0
Vehicle
30
100
HIS-388 (mg/kg)
D
**
*
HOMA-IR
50
40
30
20
10
0
Vehicle
30
100
HIS-388 (mg/kg)

Figure 2-5

Effects of HIS-388 on food intake and body weight in normal or DIO mice

In normal mice, HIS-388 (30 and 100 mg/kg) was orally administrated for 7 days. In DIO mice, HIS-388 (30 mg/kg) was orally administered for 12 days. Food intake and body weight were measured on days 0, 1, 3, 5, 7 (normal mice) or days 0, 2, 7, 12 (DIO mice). Food intake (A and C) and body weight (B and D) in normal and DIO mice are shown. Values are means ± S.E.M.. *N* = 5-9 animals per group.

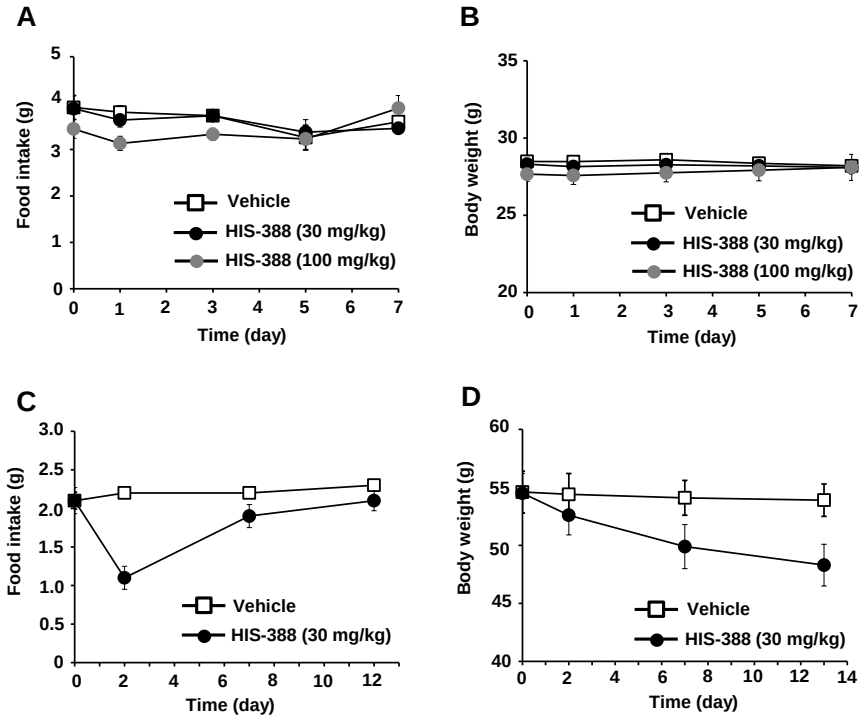
A
Food intake (g)
Time (day)
Vehicle
HIS-388 (30 mg/kg)
HIS-388 (100 mg/kg)
B
Body weight (g)
Time (day)
Vehicle
HIS-388 (30 mg/kg)
HIS-388 (100 mg/kg)
C
Food intake (g)
Time (day)
Vehicle
HIS-388 (30 mg/kg)
D
Body weight (g)
Time (day)
Vehicle
HIS-388 (30 mg/kg)

Figure 2-6

Effects of HIS-388 and pioglitazone on body weight, diabetic parameters, insulin sensitivity, and hepatic glucose production in mice with DIO

HIS-388 (30 mg/kg) and pioglitazone (PIO; 30 mg/kg) were administered orally once daily for 14 days. After the final administration, mice were deprived of food for 18 hours, and blood samples were collected for measurement of blood glucose and plasma insulin. To assess insulin sensitivity and hepatic glucose production in DIO mice, the ITT or PTT was carried out. Body weight change (A), fasting blood glucose (B), fasting plasma insulin (C), HOMA-IR index (D), blood glucose levels during ITT (E), blood glucose AUC (F) in ITT, blood glucose levels during PTT (G) and blood glucose AUC (H) in PTT are shown. Values are means ± S.E.M.. *P<0.05; **P<0.01 compared with the vehicle-treated group by t-test or Dunnett's test. N = 8 animals per group.

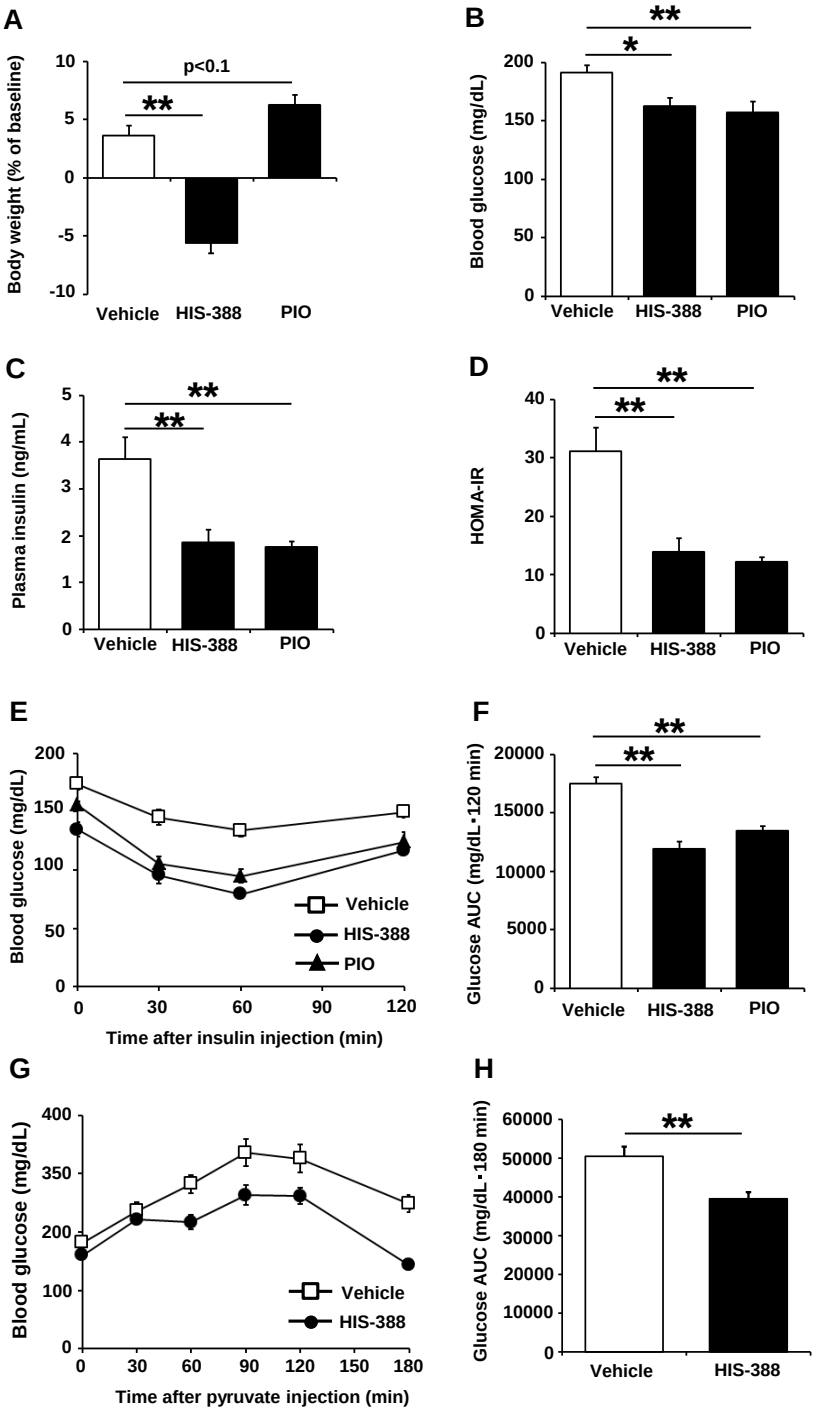
A
Body weight (% of baseline)
10
5
0
-5
-10
p<0.1
**
Vehicle
HIS-388
PIO
B
**
*
Blood glucose (mg/dL)
200
150
100
50
0
Vehicle
HIS-388
PIO
C
Plasma insulin (ng/mL)
5
4
3
2
1
0
**
**
Vehicle
HIS-388
PIO
D
HOMA-IR
40
30
20
10
0
**
**
Vehicle
HIS-388
PIO
E
Blood glucose (mg/dL)
200
150
100
50
0
Vehicle
HIS-388
PIO
0
30
60
90
120
Time after insulin injection (min)
F
Glucose AUC (mg/dL * 120 min)
20000
15000
10000
5000
0
**
**
Vehicle
HIS-388
PIO
G
Blood glucose (mg/dL)
400
350
200
100
0
Vehicle
HIS-388
0
30
60
90
120
150
180
Time after pyruvate injection (min)
H
Glucose AUC (mg/dL * 180 min)
60000
50000
40000
30000
20000
10000
0
**
Vehicle
HIS-388

Figure 2-7

Effects of HIS-388 and pioglitazone on glucose intolerance in HFD/STZ mice

Either HIS-388 (30 mg/kg) or pioglitazone (PIO; 30 mg/kg) was administered orally once daily for 15 days. After the final administration, blood samples were collected to assess the postprandial blood glucose and insulin levels. Afterward, the OGTT was carried out after 18 hours of food deprivation to determine glucose intolerance. Postprandial blood glucose (A), postprandial plasma insulin (B), blood glucose levels during OGTT (C), and blood glucose AUC (D) are shown. Values are means±S.E.M.. ***P*<0.01 compared with the vehicle-treated group by Dunnett's test; ††*P*<0.01 compared with control, STZ, HFD, and vehicle-treated groups by Turkey's test. *N*=6-8 animals per group.

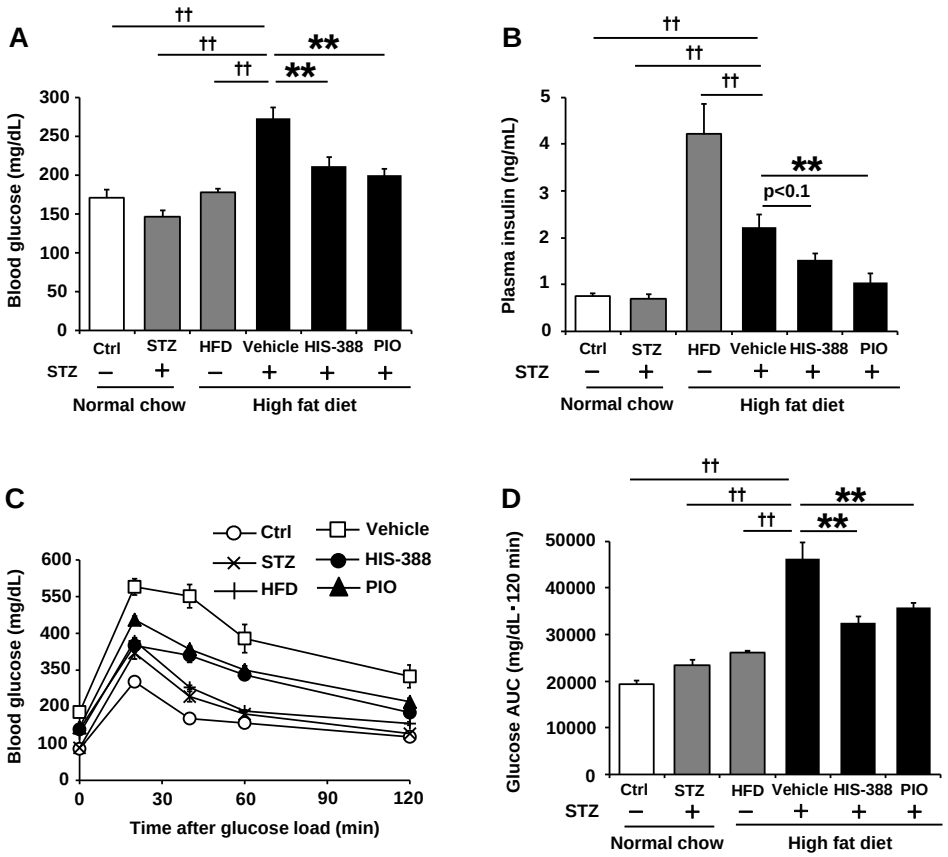
A
Blood glucose (mg/dL)
300
250
200
150
100
50
0
††
††
††
**
**
Ctrl
STZ
HFD
Vehicle
HIS-388
PIO
STZ
–
+
–
+
+
+
Normal chow
High fat diet
B
Plasma insulin (ng/mL)
5
4
3
2
1
0
††
††
††
**
p<0.1
Ctrl
STZ
HFD
Vehicle
HIS-388
PIO
STZ
–
+
–
+
+
+
Normal chow
High fat diet
C
Blood glucose (mg/dL)
600
550
400
350
200
100
0
Ctrl
STZ
HFD
Vehicle
HIS-388
PIO
0
30
60
90
120
Time after glucose load (min)
D
Glucose AUC (mg/dL * 120 min)
50000
40000
30000
20000
10000
0
††
††
††
**
**
Ctrl
STZ
HFD
Vehicle
HIS-388
PIO
STZ
–
+
–
+
+
+
Normal chow
High fat diet

General Conclusion

In chapter 1, I found that the orally active, small molecule TT01001 showed binding affinity for mitoNEET without a PPARγ activation effect. TT01001 improved diabetes and ameliorated mitochondrial function in the skeletal muscle of db/db mice without weight gain. This is the first study that demonstrates the effects of a mitoNEET ligand on glucose metabolism and mitochondrial function in a type 2 diabetic animal model. Although further study is needed to clarify the physiologic role of mitoNEET in diabetes and mitochondrial function, these findings suggest that the alteration of mitochondrial function *via* mitoNEET may be valuable for the treatment of type 2 diabetes. In chapter 2, I found that HIS-388, a novel 11β-HSD1 inhibitor, exhibited potent and long-acting 11β-HSD1 enzymatic inhibition *in vivo*. HIS-388 also ameliorated insulin sensitivity and glucose intolerance that was indistinguishable from the effects of the potent insulin sensitizer pioglitazone in DIO mice and non-genetic type 2 diabetic mice. In addition, I also found that HIS-388 has additional pharmacological effects including an antiobesity effect and an ameliorative effect on hepatic insulin resistance. These findings suggest that HIS-388, which provides potent and long-acting enzyme inhibition of 11β-HSD1, could represent a new therapeutic approach for the treatment of type 2 diabetes. Finally, these studies would support targeting mitoNEET and 11β-HSD1 as a useful therapeutic approach for the future treatment of type 2 diabetes.

Acknowledgments

I expressed my deep gratitude to all of the individuals who provided me guidance, support and encouragement during the preparation of this dissertation.

First of all, I would like to express my sincere gratitude to Prof. Kazuto Nakada, Tsukuba University for his valuable guidance, encouragement and critical advices for this Ph.D. thesis.

Next, I would like to express invaluable appreciation to my superiors in Toray Industries, Inc., Pharmaceutical Research Laboratories, Dr. Katsuhiko Iseki, Senior Director and General Manager for Pharmaceutical Research Laboratories, provided encouragement to my work. Dr. Mie Kainoh, Research Fellow, Manager of my department, also gave me enormous encouragement. Furthermore, I would like to express my special thanks to Mr. Masashi Yamamoto, Mr. Hiroki Kumagai, Dr. Tomokatsu Iwamura, Mr. Seiji Okazaki, Ms. Yumiko Sekiya, Mr. Kazutoshi Amikura, Dr. Kozue Kato, Mr. Takashi Serizawa, Ms. Kanako Serizawa, Dr. Daisuke Akazawa, Ms. Junko Kanda and Ms. Mai Yagi who helped me to study both technical and practical things as well.

Finally, it goes without saying that this thesis could not have been written without the strong support of my family.

References

Abdul-Ghani MA, Tripathy D, and DeFronzo RA (2006) Contributions of beta-cell dysfunction and insulin resistance to the pathogenesis of impaired glucose tolerance and impaired fasting glucose. Diabetes Care 29: 1130-1139.

Ahmadian M, Suh JM, Hah N, Liddle C, Atkins AR, Downes M, Evans RM (2013) PPARγ signaling and metabolism: the good, the bad and the future. Nat Med 19: 557-566.

Alberts P, Nilsson C, Selen G, Engblom LO, Edling NH, Norling S, Klingström G, Larsson C, Forsgren M, Ashkzari M, Nilsson CE, Fiedler M, Bergqvist E, Ohman B, Björkstrand E, and Abrahmsen LB (2003) Selective inhibition of 11 beta-hydroxysteroid dehydrogenase type 1 improves hepatic insulin sensitivity in hyperglycemic mice strains. Endocrinology 144: 4755-4762.

Arner P (2003) The adipocyte in insulin resistance: key molecules and the impact of thethiazolidinediones. Trends Endocrinol Metab 14: 137-145.

Anagnostis P, Katsiki N, Adamidou F, Athyros VG, Karagiannis A, Kita M, and Mikhailidis DP (2013) 11beta-Hydroxysteroid dehydrogenase type 1 inhibitors: novel agents for the treatment of metabolic syndrome and obesity-related disorders? Metabolism 62: 21-33.

Andreux PA, Houtkooper RH, Auwerx J (2013) Pharmacological approaches to restore mitochondrial function. Nat Rev Drug Discov 12: 465-483.

Bhat BG, Younis H, Herrera J, Palacio K, Pascual B, Hur G, Jessen B, Ogilvie KM, and Rejto PA (2008) Antisense inhibition of 11β-hydroxysteroid dehydrogenase type 1 improves diabetes in a novel cortisone-induced diabetic KK mouse model. Biochem Biophys Res Commun 365: 740-745.

Bieganski RM and Yarmush ML (2011) Novel ligands that target the mitochondrial membrane protein mitoNEET. J Mol Graph Model 29: 965-973.

Bogacka I, Xie H, Bray GA, Smith SR (2005) Pioglitazone induces mitochondrial biogenesis in human subcutaneous adipose tissue in vivo. Diabetes 54: 1392-1399.

Borsting E, Cheng VP, Glass CK, Vallon V, Cunard R (2012) Peroxisome proliferator-activated receptor-γ agonists repress epithelial sodium channel expression in the kidney. Am J Physiol Renal Physiol 302: F540-F551.

Brunmair B, Staniek K, Gras F, Scharf N, Althaym A, Clara R, Roden M, Gnaiger E, Nohl H, Waldhäusl W, Fürnsinn C (2004) Thiazolidinediones, like metformin, inhibit respiratory complex I. Diabetes 53: 1052-1059.

Brunton SA (2015) The potential role of sodium glucose co-transporter 2 inhibitors in the early treatment of type 2 diabetes mellitus. In J Clin Pract 69: 1071-1087.

Chomentowski P, Coen PM, Radiková Z, Goodpaster BH, Toledo FG (2011) Skeletal muscle mitochondria in insulin resistance: Differences in intermyofibrillar versus subsarcolemmal subpopulations and relationship to metabolic flexibility. J Clin Endocrinol Metab 96: 491-503.

Colca JR, McDonald WG, Waldon DJ, Leone JW, Lull JM, Bannow CA, Lund ET, Mathews WR (2004) Identification of a novel mitochondrial protein ("mitoNEET") cross-linked specifically by a thiazolidinedione photoprobe. Am J Physiol Endocrinol Metab 286: E252-E260.

Corcoran MP, Lamon-Fava S, Fielding RA (2007) Skeletal muscle lipid deposition and insulin resistance: effect of dietary fatty acids and exercise. Am J Clin Nutr 85: 662-677.

DeFronzo RA, Tobin JD, Andres R (1979) Glucose clamp technique: a method for quantifying insulin secretion and resistance. Am J Physiol 237: E214-E223.

Feinstein DL, Spagnolo A, Akar C, Weinberg G, Murphy P, Gavrilyuk V, Dello Russo C (2005) Receptor-independent actions of PPAR thiazolidinedione agonists: is mitochondrial function the key? Biochem Pharmacol 15: 177-188.

Friedman JE, Yun JS, Patel YM, and McGrane MM (1993) Glucocorticoids regulate induction of phosphoenolpyruvate carboxykinase. J Biol Chem 268: 12952-12957.

Geldenhuys WJ, Funk MO, Barnes KF, Carroll RT (2010) Structure-based design of a thiazolidinedione which targets the mitochondrial protein mitoNEET. Bioorg Med Chem Lett 20: 819-823.

Gillies PS and Dunn CJ (2000) Pioglitazone. Drugs 60: 333-343.

Harno E and White A (2010) Will treating diabetes with 11β-HSD1 inhibitors affect the HPA axis? Trends Endocrinol Metab 21: 619-627.

Holmström MH, Iglesias-Gutierrez E, Zierath JR, Garcia-Roves PM (2012) Tissue-specific control of mitochondrial respiration in obesity-related insulin resistance and diabetes. Am J Physiol Endocrinol Metab 302: E731-E739.

Hwang H, Bowen BP, Lefort N, Flynn CR, De Filippis EA, Roberts C, Smoke CC, Meyer C, Højlund K, Yi Z, Mandarino LJ (2010) Proteomics analysis of human skeletal muscle reveals novel abnormalities in obesity and type 2 diabetes. Diabetes 59: 33-42.

Hermanowski-Vosatka A, Balkovec JM, Cheng K, Chen HY, Hernandez M, Koo GC, Le Grand CB, Li Z, Metzger JM, Mundt SS, Noonan H, Nunes CN, Olson SH, Pikounis B, Ren N, Robertson N, Schaeffer JM, Shah K, Springer MS, Strack AM, Strowski M, Wu K, Wu T, Xiao J, Zhang BB, Wright SD, and Thieringer R (2005) 11beta-HSD1 inhibition ameliorates metabolic syndrome and prevents progression of atherosclerosis in mice. J Exp Med 202: 517-527.

Kadowaki T, Yamauchi T, Kubota N, Hara K, Ueki K, Tobe, K (2006) Adiponectin and adiponectin receptors in insulin resistance, diabetes, and the metabolic syndrome. J Clin Invest 116: 1784-1792.

Kahn SE, Hull RL, and Utzschneider KM (2006) Mechanisms linking obesity to insulin resistance and type 2 diabetes. Nature 444: 840-846.

Kelley DE, He J, Menshikova EV, Ritov VB (2002) Dysfunction of mitochondria in human skeletal muscle in type 2 diabetes. Diabetes 51: 2944-2950.

Kotelevtsev Y, Holmes MC, Burchell A, Houston PM, Schmoll D, Jamieson P, Best R, Brown R, Edwards CR, Seckl JR, and Mullins JJ (1997) 11beta-hydroxysteroid dehydrogenase type 1 knockout mice show attenuated glucocorticoid-inducible responses and resist hyperglycemia on obesity or stress. Proc Natl Acad Sci USA 94: 14924-14929.

Kushiro M, Takahashi Y, Ide T (2004) Species differences in the physiological activity of dietary lignan (sesamin and episesamin) in affecting hepatic fatty acid metabolism. Br J Nutr 91: 377-386.

Kusminski CM, Holland WL, Sun K, Park J, Spurgin SB, Lin Y, Askew GR, Simcox JA, McClain DA, Li C, Scherer PE (2012) MitoNEET-driven alterations in adipocyte mitochondrial activity reveal a crucial adaptive process that preserves insulin sensitivity in obesity. Nat Med 18: 1539-1549.

Lee HJ, Choi SS, Park MK, An YJ, Seo SY, Kim MC, Hong SH, Hwang TH, Kang DY, Garber AJ, and Kim DK (2002) Fenofibrate lowers abdominal and skeletal adiposity and improves insulin sensitivity in OLETF rats. Biochem Biophys Res Commun 296: 293-299.

Lee HK, Song JH, Shin CS, Park DJ, Park KS, Lee KU, Koh CS (1998) Decreased mitochondrial DNA content in peripheral blood precedes the development of non-insulin-dependent diabetes mellitus. Diabetes Res Clin Pract 42: 161-167.

Lehmann JM, Moore LB, Smith-Oliver TA, Wilkison WO, Willson TM, Kliewer SA (1995) An antidiabetic thiazolidinedione is a high affinity ligand for peroxisome proliferator-activated receptor gamma (PPAR gamma). J Biol Chem 270: 12953-12956.

Lindsay RS, Wake DJ, Nair S, Bunt J, Livingstone DE, Permana PA, Tataranni PA, and Walker BR (2003) Subcutaneous adipose 11 beta-hydroxysteroid dehydrogenase type 1 activity and

messenger ribonucleic acid levels are associated with adiposity and insulinemia in Pima Indians and Caucasians. J Clin Endocrinol Metab 88: 2738-2744.

Luo J, Quan J, Tsai J, Hobensack CK, Sullivan C, Hector R, and Reaven GM (1998) Nongenetic mouse models of non-insulin-dependent diabetes mellitus. Metabolism 47: 663-668.

Masuzaki H, Paterson J, Shinyama H, Morton NM, Mullins JJ, Seckl JR, and Flier JS (2001) A transgenic model of visceral obesity and the metabolic syndrome. Science 294: 2166-2170.

Masuzaki H, Yamamoto H, Kenyon CJ, Elmquist JK, Morton NM, Paterson JM, Shinyama H, Sharp MG, Fleming S, Mullins JJ, Seckl JR, and Flier JS (2003) Transgenic amplification of glucocorticoid action in adipose tissue causes high blood pressure in mice. J Clin Invest 112: 83-90.

Moller DE (2001) New drug targets for type 2 diabetes and the metabolic syndrome. Nature 414: 821-827.

Morton NM, Holmes MC, Fiévet C, Staels B, Tailleux A, Mullins JJ, and Seckl JR (2001) Improved lipid and lipoprotein profile, hepatic insulin sensitivity, and glucose tolerance in 11beta-hydroxysteroid dehydrogenase type 1 null mice. J Biol Chem 276: 41293-41300.

Mu J, Petrov A, Eiermann GJ, Woods J, Zhou YP, Li Z, Zycband E, Feng Y, Zhu L, Roy RS, Howard AD, Li C, Thornberry NA, and Zhang BB (2009) Inhibition of DPP-4 with sitagliptin improves glycemic control and restores islet cell mass and function in a rodent model of type 2 diabetes. Eur J Pharmacol 623: 148-154.

Nissen SE, Wolski K (2007) Effect of rosiglitazone on the risk of myocardial infarction and death from cardiovascular causes. N Engl J Med 356: 2457-2471.

Padwal R, Majumdar SR, Johnson JA, Varney J, McAlister FA (2005) A systematic review of drug therapy to delay or prevent type 2 diabetes. Diabetes Care 28: 736-744.

Pagel-Langenickel I, Bao J, Joseph JJ, Schwartz DR, Mantell BS, Xu X, Raghavachari N, Sack MN (2008) PGC-1alpha integrates insulin signaling, mitochondrial regulation, and bioenergetic function in skeletal muscle. J Biol Chem 283: 22464-22472.

Park JS, Rhee SD, Kang NS, Jung WH, Kim HY, Kim JH, Kang SK, Cheon HG, Ahn JH, and Kim KY (2011) Anti-diabetic and anti-adipogenic effects of a novel selective 11β-hydroxysteroid dehydrogenase type 1 inhibitor, 2-(3-benzoyl)-4-hydroxy-1,1-dioxo-2H-1,2-benzothiazine-2-yl-1-phenylethanone (KR-66344). Biochem Pharmacol 81: 1028-1035.

Paterson JM, Morton NM, Fievet C, Kenyon CJ, Holmes MC, Staels B, Seckl JR, and Mullins JJ (2004) Metabolic syndrome without obesity: Hepatic overexpression of 11beta-hydroxysteroid dehydrogenase type 1 in transgenic mice. Proc Natl Acad Sci USA 101: 7088-7093.

Perry RJ, Samuel VT, Petersen KF, Shulman GI (2014) The role of hepatic lipids in hepatic insulin resistance and type 2 diabetes. Nature 510: 84-91.

Phielix E, Schrauwen-Hinderling VB, Mensink M, Lenaers E, Meex R, Hoeks J, Kooi ME, Moonen-Kornips E, Sels JP, Hesselink MK, Schrauwen P (2008) Lower intrinsic ADP-stimulated mitochondrial respiration underlies in vivo mitochondrial dysfunction in muscle of male type 2 diabetic patients. Diabetes 57: 2943-2949.

Pickavance LC, Brand CL, Wassermann K, and Wilding JP (2007) The dual PPARalpha/gamma agonist, ragaglitazar, improves insulin sensitivity and metabolic profile equally with pioglitazone in diabetic and dietary obese ZDF rats. Br J Pharmacol 144: 308-314.

Quinn CE, Hamilton PK, Lockhart CJ, McVeigh GE (2008) Thiazolidinediones: effects on insulin resistance and the cardiovascular system. Br J Pharmacol 153: 636-645.

Quinlan CL, Orr AL, Perevoshchikova IV, Treberg JR, Ackrell BA, Brand MD (2012) Mitochondrial complex II can generate reactive oxygen species at high rates in both the forward and reverse reactions. J Biol Chem 287: 27255-27264.

Ritov VB, Menshikova EV, Azuma K, Wood R, Toledo FG, Goodpaster BH, Ruderman NB, Kelley DE (2010) Deficiency of electron transport chain in human skeletal muscle mitochondria in type 2 diabetes mellitus and obesity. Am J Physiol Endocrinol Metab 298: E49-E58.

Ruderman NB, Carling D, Prentki M, and Cacicedo JM (2013) AMPK, insulin resistance, and the metabolic syndrome. J Clin Invest 123: 2764-2772.

Sohn YS, Tamir S, Song L, Michaeli D, Matouk I, Conlan AR, Harir Y, Holt SH, Shulaev V, Paddock ML, Hochberg A, Cabanchick IZ, Onuchic JN, Jennings PA, Nechushtai R, Mittler R (2013) NAF-1 and mitoNEET are central to human breast cancer proliferation by maintaining mitochondrial homeostasis and promoting tumor growth. Proc Natl Acad Sci USA 110: 14676-14681.

Song J, Oh JY, Sung YA, Pak YK, Park KS, Lee HK (2001) Peripheral blood mitochondrial DNA content is related to insulin sensitivity in offspring of type 2 diabetic patients. Diabetes Care 24: 865-869.

Spinazzi M, Casarin A, Pertegato V, Salviati L, Angelini C (2012) Assessment of mitochondrial respiratory chain enzymatic activities on tissues and cultured cells. Nat Protoc 31: 1235-1246.

Sundbom M, Kaiser C, Björkstrand E, Castro VM, Larsson C, Selén G, Nyhem CS, and James SR (2008) Inhibition of 11betaHSD1 with the S-phenylethylaminothiazolone BVT116429 increases adiponectin concentrations and improves glucose homeostasis in diabetic KKAy mice. BMC Pharmacol 8: 3.

Suzuki A Yasuno T Kojo H, Hirosumi J, Mutoh S, Notsu Y (2000) Alteration in expression profiles of a series of diabetes-related genes in db/db mice following treatment with thiazolidinediones. Jpn J Pharmacol 84: 113-23.

Tang WH and Maroo A (2007) PPARgamma agonists: safety issues in heart failure. Diabetes Obes Metab 9: 447-454.

Turner N, Bruce CR, Beale SM, Hoehn KL, So T, Rolph MS, Cooney GJ (2007) Excess lipid availability increases mitochondrial fatty acid oxidative capacity in muscle: evidence against a role for reduced fatty acid oxidation in lipid-induced insulin resistance in rodents. Diabetes 56: 2085-2092.

van Belle TL, Coppieters KT, von Herrath MG (2011) Type 1 diabetes: etiology, immunology, and therapeutic strategies. Physiol Rev 91: 79-118.

Wang SJ, Birtles S, de Schoolmeester J, Swales J, Moody G, Hislop D, O'Dowd J, Smith DM, Turnbull AV, Arch JR (2006) Inhibition of 11beta-hydroxysteroid dehydrogenase type 1 reduces food intake and weight gain but maintains energy expenditure in diet-induced obese mice. Diabetologia 49: 1333-1337.

Whiting DR, Guariguata L, Weil C, and Shaw J (2011) IDF diabetes atlas: global estimates of the prevalence of diabetes for 2011 and 2030. Diabetes Res Clin Pract 94: 311-321.

Wiley SE, Murphy AN, Ross SA, van der Geer P, Dixon JE (2007) MitoNEET is an iron-containing outer mitochondrial membrane protein that regulates oxidative capacity. Proc Natl Acad Sci USA 104: 5318-5323.

Zuris JA, Harir Y, Conlan AR, Shvartsman M, Michaeli D, Tamir S, Paddock ML, Onuchic JN, Mittler R, Cabantchik ZI, Jennings PA, Nechushtai R (2011) Facile transfer of [2Fe-2S] clusters from the diabetes drug target mitoNEET to an apo-acceptor protein. Proc Natl Acad Sci USA 108: 13047-13052.